MASSACHUSETTS INSTITUTE OF TECHNOLOGY
LINCOLN LABORATORY

ACCURACY LIMITATIONS OF RANGE-RANGE (SPHERICAL) MULTILATERATION SYSTEMS

H. B. LEE

TECHNICAL NOTE 1973-43

11 OCT 1973

LEXINGTON MASSACHUSETTS

TECHNICAL REPORT STANDARD TITLE PAGE

1. Report No.	2. Government Accession No.	3. Recipient's Catalog No.
DOT/TSC-RA-3-8-(1)		

4. Title and Subtitle	5. Report Date
Accuracy Limitations of Range-Range (Spherical) Multilateration Systems	11 October 1973
	6. Performing Organization Code

7. Author(s)	8. Performing Organization Report No.
Harry B. Lee	Technical Note 1973-43

9. Performing Organization Name and Address	10. Work Unit No.
Massachusetts Institute of Technology Lincoln Laboratory P.O. Box 73 Lexington, Massachusetts 02173	11. Contract or Grant No. DOT/TSC-RA-3-8 Task 1
	13. Type of Report and Period Covered Technical Note
12. Sponsoring Agency Name and Address Transportation Systems Center Department of Transportation Cambridge, Massachusetts	14. Sponsoring Agency Code

15. Supplementary Notes

The work reported in this document was performed at Lincoln Laboratory, a center for research operated by Massachusetts Institute of Technology.

16. Abstract

This report presents a novel procedure for determining the accuracy of range-range (or spherical) multilateration systems. The procedure is a generalization of one previously described for hyperbolic multilateration systems [1].

A central result is a demonstration that the inverse of the covariance matrix for positional errors corresponds to the moment of inertia matrix of a simple mass configuration. The insight afforded by this fact is used to resolve a number of questions relating to accuracy. Specific questions addressed include the following:

1. How does accuracy depend upon the number of receivers?
2. How does accuracy depend upon the deployment of receivers?
3. What is the maximum accuracy that can be obtained from N receivers? How should the receivers be deployed to maximize accuracy?
4. How do altitude errors compare to horizontal errors in satellite-based systems? In ground-based systems?

17. Key Words	18. Distribution Statement
aircraft surveillance navigation position determination range-range least squares estimation multilateration geometric dilution of precision	Availability is unlimited. Document may be released to the National Technical Information Service, Springfield, Virginia 22151, for sale to the public.

19. Security Classif. (of this report)	20. Security Classif. (of this page)	21. No. of Pages	22. Price
Unclassified	Unclassified	112	4.25 HC 1.45 MF

Form DOT F 1700.7 (8-69)

CONTENTS

CONTENTS (Continued)

I. INTRODUCTION

This note deals with the accuracy of range-range or spherical multilateration systems. Specifically the note extends a number of useful results recently developed for hyperbolic multilateration systems [1] to spherical systems.

Spherical systems operate by utilizing measurements of range from a number of stations to a subject (i.e., an aircraft), the position of which is to be determined. Each range measurement serves to localize the subject to a sphere centered about one of the stations. Thus the subject's position is determined by calculating the common intersection point of the spheres.

An example of a satellite-based spherical navigation system is shown in Figure 1.1. The system operates as follows. At an agreed upon time, satellites 1,2,..,N transmit distinct pulses. The pulse time of arrivals (TOA's) at the aircraft are read from a local clock. The known transmission time is subtracted from the TOA's, and the resulting time differences (equivalent to ranges) are used to calculate the aircraft position.

An example of a ground-based spherical system is shown in Figure 1.2. The system operates as follows. The ground-based stations transmit pulses to the aircraft. The aircraft transponder retransmits the pulses which are picked up by the originating stations. The resulting round trip times (proportional to range) are used to calculate the aircraft position.

The accuracy of such systems is limited by the accuracy with which the locations of the transmitting stations are known, by propagation disturbances in the atmosphere, by noise disturbances in the receiver(s), and the accuracy of the clocks used. Typically, the algorithm that calculates position translates these errors into corresponding aircraft position errors.

Considerable previous work [2-9] has been done on calculating the accuracy of such systems. Thus, given disturbance statistics and a specific deployment of transmitters and receivers, it is straightforward to calculate the resulting positional error.

The purpose of this note is to present a novel method for calculating the accuracy of a spherical multilateration system, and then to use the method as a basis for drawing some general conclusions about accuracy. Thus, in contrast to the referenced work [2-9], the emphasis is not on calculating accuracy measures for specific deployments of transmitters and receivers. Rather the emphasis is on identifying general properties of spherical multilateration systems. Thus, for example, the report addresses questions such as the following:

1. What are the trade-offs between accuracy and the number of transmitting (or receiving) stations?
2. What are the trade-offs between accuracy and the deployment of transmitting (or receiving) stations?
3. How do the errors depend on direction? (E.g., in an aircraft surveillance system it is desirable that altitude errors be smaller than horizontal errors; is this the case?)
4. How does accuracy depend upon the accuracy of the clock used to record signal arrival times?
5. What are the smallest rms errors that can be attained using a fixed number of receivers? How should the receivers be deployed to achieve minimum error?

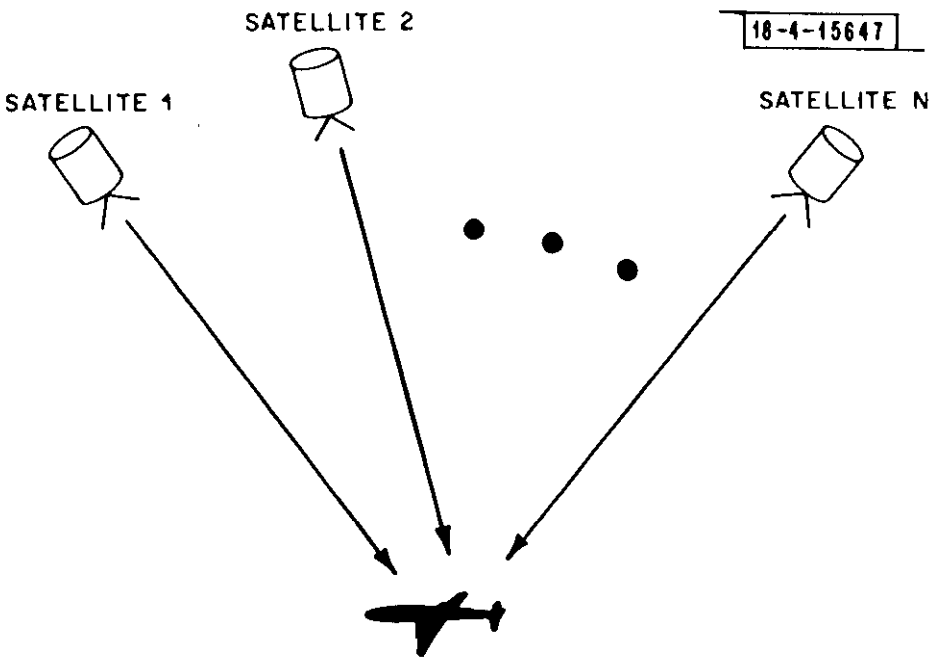

Figure 1.1

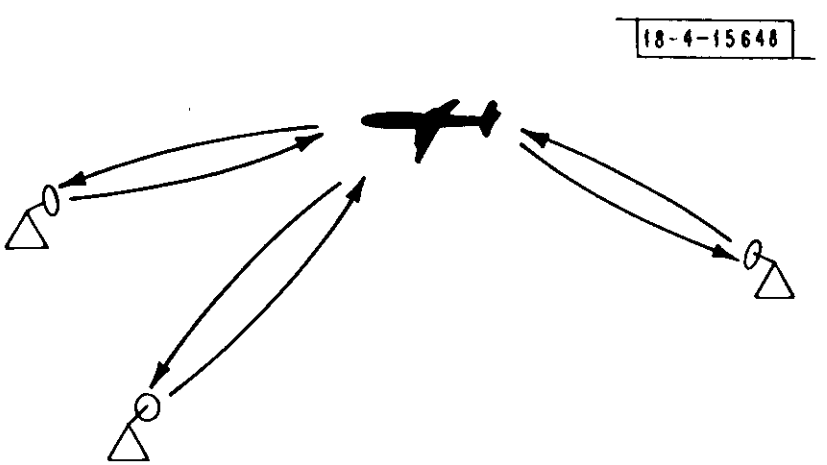

Figure 1.2

II. SUMMARY OF RESULTS

Although the present work has been motivated by satellite-based multilateration systems like that shown in Figure 1.1, the work is reported in more general terms to make the results available to other applications as well. Thus, it is assumed that a spherical multilateration system consists of a number N of beacons (e.g., satellite-based transmitters), and a subject (e.g., an aircraft). The beacons and the subject are assumed to be in fixed positions. The beacons simultaneously transmit signals that are received at different times by the subject (or equivalently, the beacons simultaneously transmit a signal that is transponded by the subject back to the beacons). Due to disturbances of various kinds, the TOAs are somewhat in error. As a result, the calculated subject position is correspondingly in error.

The report treats both satellite-based and ground-based systems. It should be noted that the assumption of fixed beacon positions ignores the effects of motion in satellite-based systems. Thus with regard to such systems, the results apply to a single instant of time.

In some cases, no geometrical constraints are placed upon the beacon locations. In other cases, the beacons are assumed to be confined to a viewing cone, or a cone-complement.

The main results are as follows:

1. It is shown that the inverse of the covariance matrix for positional error corresponds to the moment of inertia matrix for a simple mass configuration. The insight provided by this fact makes it possible to answer many questions relating to accuracy [Section VIII].

2. The performance of an actual spherical multilateration system is bounded by the performance of a comparable hyperbolic system and that of an "ideal" spherical system (defined in

Section X). Specifically, the accuracy of a spherical system always exceeds that of a hyperbolic system, but is not as good as that of an ideal system [Section X].

3. If σ_0 denotes the rms error in the recorded signal arrival times due to highly correlated effects (e.g., clock error, ionospheric delays, transponder delay), and σ_t denoes the corresponding error due to uncorrelated effects (e.g., receiver noise, beacon location errors), then the accuracy benefits of an ideal spherical system are obtained if $\sigma_0 < \sigma_t/\sqrt{N}$ where N denotes the number of beacons. For $\sigma_0 > \sigma_t/\sqrt{N}$ accuracy begins to degrade, and approaches that of a hyperbolic system as σ_0 becomes large [Sections XV and XVIII].

4. For both satellite-based and ground-based systems it is shown that error measures typically are not highly sensitive to the number N of beacons. Specifically, typical error measures are proportional to $1/\sqrt{N}$. Thus, for example, to double system accuracy by the expedient of adding beacons, it is necessary to increase the number of beacons by a factor of four [Sections XIII, XIV, XVI, and XVII].

5. The accuracy of an ideal spherical system is much more sensitive to beacon deployment. For example, in the case of N beacons distributed uniformly within a viewing cone, increasing the cone half angle from $\phi = 30°$ to $\phi = 60°$ doubles accuracy, an improvement that otherwise would require a fourfold increase in the number of beacons [Section XIII].

6. For satellite-based systems the errors made using ideal spherical multilateration are primarily horizontal errors. Typically rms horizontal errors are twice as large as rms altitude errors [Section XIII].

7. By contrast, for ground-based systems the errors are primarily altitude errors [Section XVI].

8. Expressions are derived for the minimum rms error that can be expected from N beacons using ideal spherical multilateration. Corresponding optimum beacon deployments also are presented. The results assume that the beacon locations either are unrestricted, or are restricted to a viewing cone of arbitrary half angle [Section XX].

9. The moment of inertia method for caculating the inverse of the error covariance matrix is generalized to accommodate an independent (e.g., barometric) altitude measurement [Section XIX].

All results are derived for the three-dimensional position determination problem. Corresponding results hold for the two-dimensional problem as well. The derivations parallel those given here.

III. TIME OF ARRIVAL EQUATIONS

A typical spherical multilateration system is shown in Figure 3.1. Under ideal conditions the signal arrival times are related to the distances $d_1, d_2, \ldots, d_N$ as follows:

$$\begin{aligned} t_1 &= t_0 + d_1/c \\ t_2 &= t_0 + d_2/c \\ &\vdots \\ t_N &= t_0 + d_N/c \end{aligned} \tag{3.1}$$

where

t_j = The time of arrival (TOA) of the pulse from the jth beacon ($j = 1,2,\ldots N$).

t_0 = The time of pulse transmission.

d_j/c = The transit time from the jth beacon to the subject (c denotes the signal velocity).

The basic procedure for determining the subject position from (3.1) consists of expressing the distances d_j in terms of some convenient coordinate system, and then solving (3.1) for the subject coordinates. Note that the system of Equations (3.1) is overdetermined in that it consists of N equations in 3 unknowns. Thus, if no measurement errors are present, only three of the equations are needed to calculate subject position. The remaining equations are redundant. When the data contains measurement errors, however, it is advantageous to use the entire system of equations to calculate subject position. Specifically, it

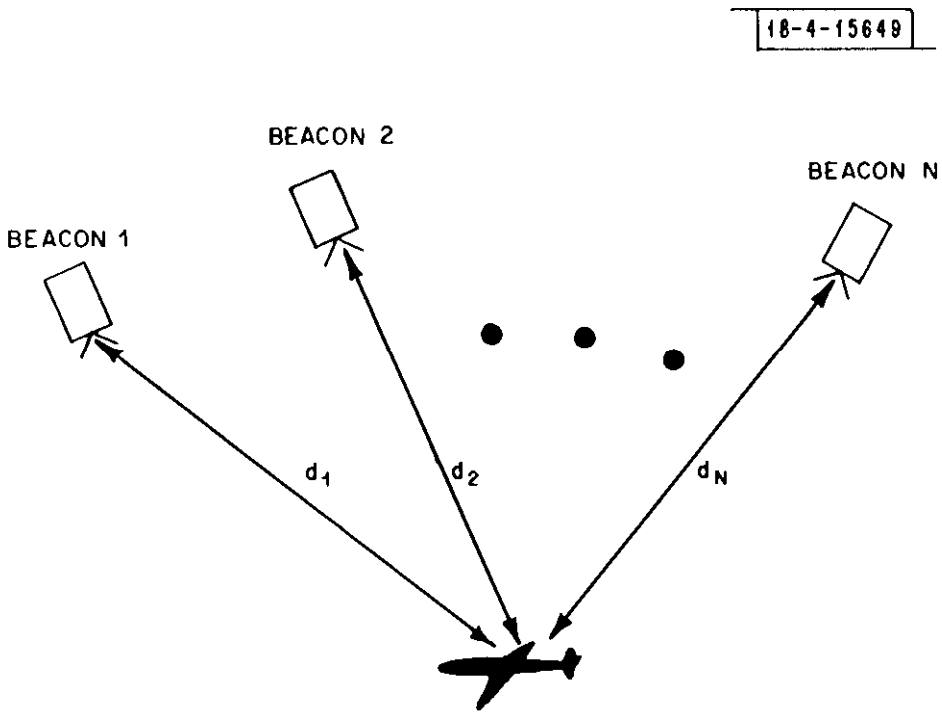

Figure 3.1

is desirable to average the system of equations together to obtain a set of three equations in three unknowns, and then solve the resulting equations for the subject position. The averaging step improves final accuracy in that it permits error cancellation among the measured data.

Equation (3.1) makes the following idealizing assumptions:

1. The time of signal transmission is exactly known.
2. Signal propagation is ideal.
3. No errors are made in measuring the arrival times of the signals.

If conditions 1-3 are satisfied the subject's position relative to the beacons can be determined exactly by solving Equations (3.1) for the coordinates of the subject. If in addition,

4. The beacon positions are exactly known in an earth-based reference frame

the position of the subject relative to a point on earth can be determined exactly.

Conditions 1-4 never are satisfied, however. The measured quantities that appear in (3.1) always are in error. Thus the relative position of the subject that is calculated from the system of Equations (3.1) is correspondingly in error, as is the position calculated in an earth reference frame.

IV. SOURCES OF ERROR

The quantities t_j, t_0, and d_j that appear in (3.1) are ideal quantities in the sense that they are not available for calculation. Thus let t_j^*, t_0^*, and d_j^* denote the corresponding quantities that are available for calculation. That is, let

t_j^* = The measured TOA from the j^{th} beacon (j=1,2,...,N).

t_0^* = The measured (or estimated) time of signal transmission.

d_j^* = The measured (or estimated) distance from the j^{th} beacon to the subject.

The quantities t_j^*, t_0^*, and d_j^* are related to their ideal counterparts t_j, t_0, and d_j as follows:

$$t_j^* = t_j + \Delta t_j \qquad [j=1,2,\ldots,N] \tag{4.1}$$

$$t_0^* = t_0 + \Delta t_0 \tag{4.2}$$

$$d_j^* = d_j + \Delta d_j \tag{4.3}$$

where Δt_j, Δt_0, and Δd_j denote the relevant measurement (or estimation) errors.

For present purposes it is assumed that the time of arrival error Δt_j has four principal components. These are as follows:

$\Delta t_{j,1}$ = An approximately uniform delay imposed upon all N signals (e.g., by the ionosphere, or a transponder).

$\Delta t_{j,2}$ = Fluctuation in the transit time of the jth signal due to random effects in the propagation media.

$\Delta t_{j,3}$ = Error in the measured TOA of the jth signal due to receiver noise.

$\Delta t_{j,4}$ = Error in the measured TOA of the jth signal due to clock error.

The error Δt_j therefore can be expressed as follows:

$$\Delta t_j = \sum_{k=1}^{4} \Delta t_{j,k} \tag{4.4}$$

The error Δt_0 results from inaccuracies in the clock used to measure t_0, or from error in the assumed time of signal transmission (if t_0 is estimated rather than measured).

In satellite applications the error Δd_j represents combined measurement and tracking errors. In ground-based applications Δd_j corresponds to the beacon siting error.

It is reasonable to expect that all of the foregoing errors have zero mean over a large number of measurements with different transmitting and receiving equipment, with the exception of $\Delta t_{j,1}$. The uniform delay $\Delta t_{j,1}$ imposed by the ionosphere, or a transponder has a definite non-zero mean that is measurable, and that can be subtracted from the arrival times t_j^* before the subject position is calculated. The viewpoint taken here is that this correction has been made. Thus, in what follows, it is assumed that

A1. <u>All</u> of the errors $\Delta t_{j,1}..,\Delta t_{j,4}$, Δt_0 and Δd_j have zero mean, and that $\Delta t_{j,1}$ denotes the residual deviation of the uniform delay from its mean.

With regard to correlation of the errors, observe that each type of error tends to fall into one of the following categories.

I. The error is generated by uncorrelated physical mechanisms for different j. Thus the errors for different j are statistically independent.

II. The error is generated by highly correlated (if not identical) physical mechanisms for different j. Thus the errors for different j tend to have correlation coefficients of unity.

Table 4.1 indicates the appropriate category for each error source. Note that the clock error $\Delta t_{j,4}$ can be of either type. If independent clocks are used to measure TOAs, then the errors $\Delta t_{j,4}$ belong in Category I. If the same clock is used to measure all TOAs, the $\Delta t_{j,4}$ belong to Category II.

Henceforth, the following assumptions are made concerning correlation of errors.

Error Correlation Assumptions

A2. Pairs of errors that appear in different rows of Table 4.1 are uncorrelated.

A3. Pairs of like Category I errors are uncorrelated for different j. For example, $\Delta t_{1,2}$ and $\Delta t_{2,2}$ are uncorrelated.

A4. Pairs of like Category II errors have identical variances, and a correlation coefficient of unity. For example, $\Delta t_{1,1}$ and $\Delta t_{2,1}$ have identical variances and a unit correlation coefficient.

Table 4.1

Error	Category I (Independent for different j)	Category II (Unity Correlated for different j)
$\Delta t_{j,1}$ (residual delay)		X
$\Delta t_{j,2}$ (transit time fluctuation)	X	
$\Delta t_{j,3}$ (receiver noise)	X	
$\Delta t_{j,4}$ (clock error)	X or	X
Δt_0 (transmission time error)		X
Δd_j (beacon position error)	X	

V. SUMMARY ERROR VARIABLES

Use of (4.1) - (4.3) to eliminate the ideal quantities t_0, t_j and d_j from (3.1) produces the following equations for the measurable quantities t_j^*, t_0^*, and d_j^*.

$$\begin{aligned} t_1^* &= t_0^* + d_1^*/c + \Delta t_1 - \Delta t_0 - \Delta d_1/c \\ &\vdots \\ t_N^* &= t_0^* + d_N^*/c + \Delta t_N - \Delta t_0 - \Delta d_N/c \end{aligned} \tag{5.1}$$

Equation (5.1) can be expanded to place in evidence the TOA error components $\Delta t_{j,1}..,\Delta t_{j,4}$ by substituting (4.4) in (5.1). The resulting equations are

$$\begin{aligned} t_1^* &= t_0^* + d_1^*/c + \sum_{k=1}^{4} \Delta t_{1,k} - \Delta t_0 - \Delta d_1/c \\ &\vdots \\ t_N^* &= t_0^* + d_N^*/c + \sum_{k=1}^{4} \Delta t_{N,k} - \Delta t_0 - \Delta d_N/c \end{aligned} \tag{5.2}$$

To simplify subsequent discussions it is convenient to define <u>summary error variables</u> as follows:

$$\varepsilon_0 = \Delta t_{j,1} + \left\{\Delta t_{j,4}\right\}_{II} - \Delta t_0 \tag{5.3}$$

$$\varepsilon_j = \Delta t_{j,2} + \Delta t_{j,3} + \left\{\Delta t_{j,4}\right\}_{I} - \Delta d_j/c \tag{5.4}$$

The error ε_0 is the sum of all errors that are unity correlated [see Table 4.1]. The ε_j (j = 1,2,...,N) are sums of the uncorrelated errors for the different signal paths. The notations $\{\ \}_I$ and $\{\ \}_{II}$ mean that $\Delta t_{j,4}$ belongs in (5.4) if $\Delta t_{j,4}$ falls in Category I, and belongs in (5.3) if $\Delta t_{j,4}$ falls in Category II.

Equations (5.2) take the following simple form when rewritten in terms of the $\varepsilon_0,\varepsilon_1,\ldots,\varepsilon_N$

$$\begin{aligned} t_1^* &= t_0^* + d_1^*/c + \varepsilon_0 + \varepsilon_1 \\ &\vdots \\ t_N^* &= t_0^* + d_N^*/c + \varepsilon_0 + \varepsilon_N \end{aligned} \tag{5.5}$$

All subsequent discussion is carried out in terms of the summary error variables $\varepsilon_0,\varepsilon_1,\ldots,\varepsilon_N$. No further mention is made of the constituent errors in Table 4.1. Henceforth, the error ε_0 is called the clock error, even though other errors also contribute to it. The errors ε_j multiplied by the velocity c of signal propagation are called ranging errors.

As a result of assumptions A1-A4 of Section IV, it is assumed that $\varepsilon_0,\varepsilon_1,\ldots,\varepsilon_N$ are zero mean random variables with the diagonal covariance matrix

$$\underline{P}_{\varepsilon} = \begin{bmatrix} \sigma_0^2 & & 0 \\ & \sigma_1^2 & \\ & & \ddots \\ 0 & & \sigma_N^2 \end{bmatrix} \tag{5.6}$$

The covariance matrix $\underline{P}_\Sigma$ for the error terms $(\varepsilon_0 + \varepsilon_j)$ in (5.5) can be expressed in terms of $\underline{P}_\varepsilon$ as follows:

$$\underline{P}_\Sigma = E\left\{\begin{bmatrix}(\varepsilon_0 + \varepsilon_1)\\ \cdot\\ \cdot\\ \cdot\\ (\varepsilon_0 + \varepsilon_N)\end{bmatrix}\left[(\varepsilon_0 + \varepsilon_1), \ \ldots \ (\varepsilon_0 + \varepsilon_N)\right]\right\}$$

$$= E\{(\underline{H}\ \underline{\varepsilon})\ (\underline{H}\ \underline{\varepsilon})'\}$$

$$= \underline{H}\ \underline{P}_\varepsilon\ \underline{H}' \qquad (5.7)$$

where E denotes expectation,

$$\underline{\varepsilon} = \begin{bmatrix}\varepsilon_0\\ \varepsilon_1\\ \cdot\\ \cdot\\ \varepsilon_N\end{bmatrix} \Big\} (N + 1) \text{ rows} \qquad (5.8)$$

and

$\underline{H}$ = an N x (N+1) matrix of the form

$$\begin{bmatrix}1 & 1 & & & \\ 1 & & 1 & & \\ \cdot & & & \cdot & \\ \cdot & & & & \\ 1 & & & & 1\end{bmatrix} \Big\} \text{N rows} \qquad (5.9)$$

$\underbrace{\qquad\qquad\qquad}_{(N + 1) \text{ columns}}$

VI. POSITIONAL ERRORS WITH OPTIMAL PROCESSING

Let $\underline{R}$ be a (3x1) vector that specifies the actual subject position. A number of different methods exist for "solving" the TOA Equation (5.5) for $\underline{R}$. Each method can be viewed as defining a (3x1) vector function (estimator)

$$\hat{\underline{R}} = \underline{f}(t_1^*, t_2^*, \ldots, t_N^*;\ t_0^*;\ d_1^*, d_2^*, \ldots, d_N^*) \tag{6.1}$$

that approximates $\underline{R}$.

The generalized least squares procedure is one such method [4,6,8]. The procedure involves linearizing the TOA equations about a point known to be near the subject. The subject position $\underline{R}$ relative to the reference point then is approximated by the vector $\hat{\underline{R}}$ that minimizes the quadratic error measure

$$Q = [(\varepsilon_0 + \varepsilon_1), \ldots, (\varepsilon_0 + \varepsilon_N)] \begin{bmatrix} & & \\ & \underline{P_\Sigma^{-1}} & \\ & & \end{bmatrix} \begin{bmatrix} (\varepsilon_0 + \varepsilon_1) \\ (\varepsilon_0 + \varepsilon_2) \\ \vdots \\ (\varepsilon_0 + \varepsilon_N) \end{bmatrix}$$

$$= (\underline{H}\ \underline{\varepsilon})'\ \underline{P_\Sigma^{-1}}(\underline{H}\ \underline{\varepsilon}) \tag{6.2}$$

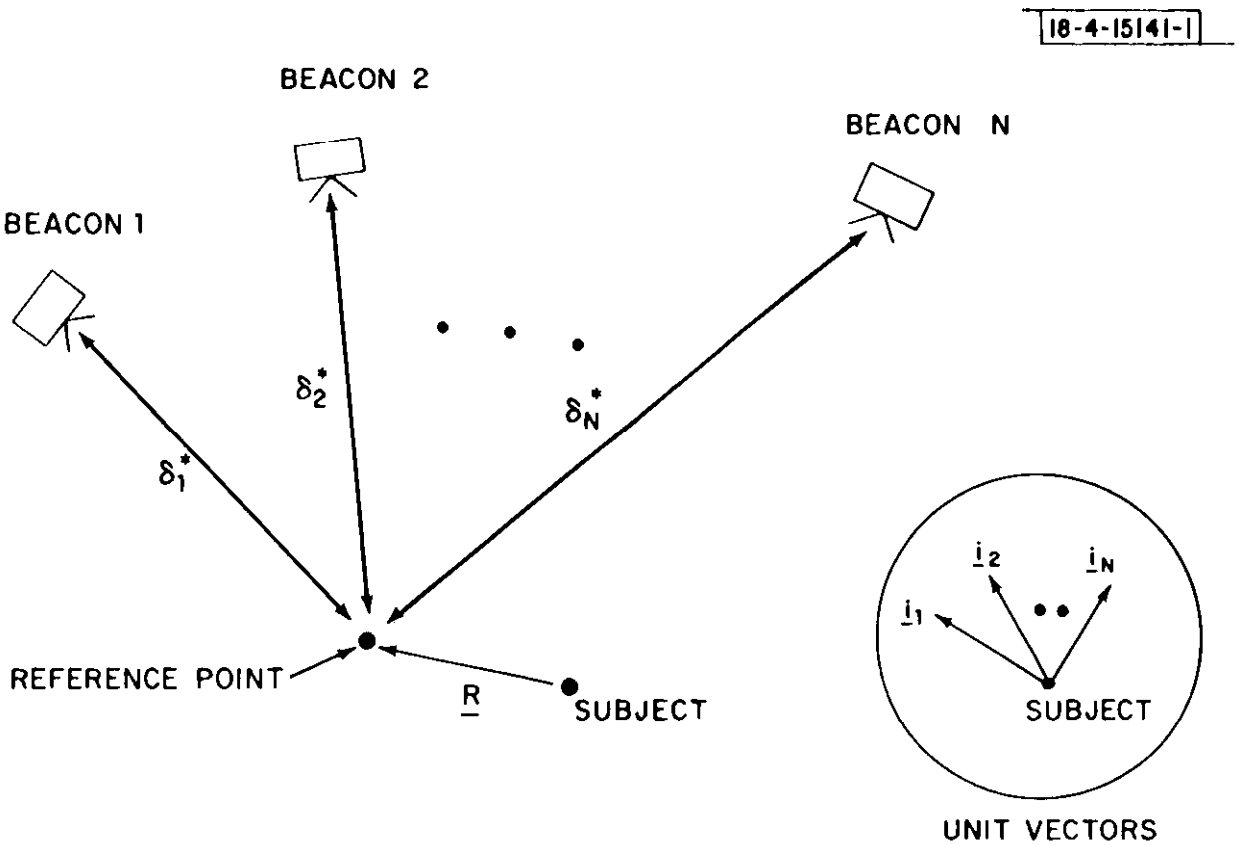
18-4-15141-1
BEACON 2
BEACON N
BEACON 1
δ_2^*
δ_N^*
δ_1^*
REFERENCE POINT
$\underline{R}$
SUBJECT
$\underline{i}_2$
$\underline{i}_N$
$\underline{i}_1$
SUBJECT
UNIT VECTORS

Figure 6.1

The linearized equations take the following form:

$$t_1^* = \frac{1}{c}\,\delta_1^* + \frac{1}{c}\,\underline{i}_1 \cdot \underline{R} + (\varepsilon_0 + \varepsilon_1)$$

$$\vdots$$

$$t_N^* = \frac{1}{c}\,\delta_N^* + \frac{1}{c}\,\underline{i}_N \cdot \underline{R} + (\varepsilon_0 + \varepsilon_N) \qquad (6.3)$$

where

δ_j^* = The distance from the assumed position of the jth beacon to the reference point.

$\underline{i}_j$ = A (1x3) unit vector pointing from the subject to the jth satellite; see Figure 6.1.

$\underline{R}$ = A (3x1) vector specifying the subject position relative to the reference point; see Figure 6.1.

For the purpose of minimizing (6.2) it is convenient to rewrite Equations (6.3) in matrix notation as follows:

$$\underline{T}^* = \frac{1}{c}\,\underline{\delta}^* + \frac{1}{c}\,\underline{H}\,\underline{F} \cdot \underline{R} + \underline{H}\,\underline{\varepsilon} \qquad (6.4)$$

where

$$\underline{T}^* = \begin{bmatrix} t_1^* \\ \vdots \\ t_N^* \end{bmatrix}, \qquad \underline{\delta}^* = \begin{bmatrix} \delta_1^* \\ \vdots \\ \delta_N^* \end{bmatrix} \qquad (6.5,6.6)$$

$$\underline{F} = \underbrace{\begin{bmatrix} \underline{0} \\ \underline{i}_1 \\ \vdots \\ \underline{i}_N \end{bmatrix}}_{3 \text{ columns}} \Bigg\} (N + 1) \text{ rows} \qquad (6.7)$$

and where $\underline{H}$ and $\underline{\varepsilon}$ are given by (5.9) and (5.8).

Use of (6.4) in (6.2) yields

$$Q(\underline{R}) = [\underline{T}^* - \frac{1}{c}\underline{\delta}^* - \frac{1}{c}\underline{H}\,\underline{F}\cdot\underline{R}]'\,\underline{P}_{\Sigma}^{-1}[\underline{T}^* - \frac{1}{c}\underline{\delta}^* - \frac{1}{c}\underline{H}\,\underline{F}\,\underline{R}] \qquad (6.8)$$

The minimizing condition that

$$dQ = -\frac{2}{c}\underline{dR}'\,\underline{F}'\,\underline{H}'\,\underline{P}_{\Sigma}^{-1}[\underline{T}^* - \frac{1}{c}\underline{\delta}^* - \frac{1}{c}\underline{H}\,\underline{F}\,\underline{R}] \qquad (6.9)$$

equal zero for all vector differentials $\underline{dR}$ requires that

$$\underline{0} = \underline{F}'\,\underline{H}'\,\underline{P}_{\Sigma}^{-1}[\underline{T}^* - \frac{1}{c}\underline{\delta}^* - \frac{1}{c}\underline{H}\,\underline{F}\,\underline{R}] \qquad (6.10)$$

Solution of (6.10) produces the estimator

$$\hat{\underline{R}} = [\underline{F}'\,\underline{H}'\,\underline{P}_{\Sigma}^{-1}\,\underline{H}\,\underline{F}]^{-1}\,\underline{F}'\,\underline{H}'\,\underline{P}_{\Sigma}^{-1}[c\underline{T}^* - \underline{\delta}^*] \qquad (6.11)$$

Use of (6.4) in (6.11) shows that the error $\hat{\underline{R}} - \underline{R}$ in calculated position is related to $\underline{\varepsilon}$ as follows:

$$\hat{\underline{R}} - \underline{R} = c[\underline{F}'\,\underline{H}'\,\underline{P}_{\Sigma}^{-1}\,\underline{H}\,\underline{F}]^{-1}\,\underline{F}'\,\underline{H}'\,\underline{P}_{\Sigma}^{-1}\,\underline{H}\,\underline{\varepsilon} \qquad (6.12)$$

Clearly, $\hat{\underline{R}} - \underline{R} = 0$ if $\underline{\varepsilon} = 0$. More generally $E[\hat{\underline{R}} - \underline{R}] = 0$ provided $E[\underline{\varepsilon}] = 0$. Therefore, the estimator (6.11) is unbiased. The associated covariance matrix for the error $\hat{\underline{R}} - \underline{R}$ is as follows:

$$\begin{aligned}\underline{P}_{\Delta R} &= E[(\hat{\underline{R}} - \underline{R})\,(\hat{\underline{R}} - \underline{R})'] \\ &= c^2[\underline{F}'\,\underline{H}'\,\underline{P}_{\Sigma}^{-1}\,\underline{H}\,\underline{F}]^{-1} \\ &= c^2[\underline{F}'\,\underline{H}'(\underline{H}\,\underline{P}_{\varepsilon}\,\underline{H}')^{-1}\,\underline{H}\,\underline{F}]^{-1} \qquad (6.13)\end{aligned}$$

The least squares result (6.11) represents only one possible estimator of the subject position $\underline{R}$. Other workable estimators can readily be devised. According to Markov's Theorem [10], however, the generalized least squares estimator is optimal in the sense that it produces the smallest mean-square error of all estimators that satisfy the following (weak) conditions.

Conditions

1. The estimator is unbiased.
2. For the error magnitudes of interest, the estimator is linear in the ε_j. That is

$$\hat{\underline{R}} = \underline{R} + \underline{A}\,\underline{\varepsilon}$$

where the matrix $\underline{A}$ is independent of the ε_j.

Accordingly, in what follows, we restrict attention to the errors generated by the least squares procedure.

VII. ERROR MEASURES

For the purpose of assessing accuracy it is convenient to rewrite the covariance matrix (6.13) as follows:

$$\underline{P}_{\Delta R} = (\sigma^* c)^2 \, \underline{\Gamma} \tag{7.1}$$

$$= (\sigma^* c)^2 \begin{bmatrix} \Gamma_{xx} & \Gamma_{xy} & \Gamma_{xz} \\ \Gamma_{xy} & \Gamma_{yy} & \Gamma_{zy} \\ \Gamma_{xz} & \Gamma_{zy} & \Gamma_{zz} \end{bmatrix} \tag{7.2}$$

where $(\sigma^* c)^2$ denotes the mean-squared ranging error. That is

$$(\sigma^* c)^2 = \frac{1}{N} \sum_{j=1}^{N} (\sigma_j c)^2 \tag{7.3}$$

Use of (6.13) in (7.1) shows that the $\underline{\Gamma}$ matrix is defined by the relationship

$$\underline{\Gamma} = \frac{1}{(\sigma^*)^2} [\underline{F}' \, \underline{H}' (\underline{H} \, \underline{P}_\epsilon \, \underline{H}')^{-1} \, \underline{H} \, \underline{F}]^{-1}$$

$$= [\underline{F}' \, \underline{H}' (\underline{H} \, \underline{P}_n \, \underline{H}')^{-1} \, \underline{H} \, \underline{F}]^{-1} \tag{7.4}$$

where $\underline{P}_n$ denotes the normalized covariance matrix

$$\underline{P}_n = \begin{bmatrix} (\frac{\sigma_0}{\sigma^*})^2 & & 0 \\ & (\frac{\sigma_1}{\sigma^*})^2 & \\ 0 & & \ddots \\ & & (\frac{\sigma_N}{\sigma^*})^2 \end{bmatrix} \tag{7.5}$$

All of the conventional measures of accuracy are directly available from the diagonal elements of the covariance matrix (7.2). For example, the mean-squared errors in the X', Y'and Z'directions are given respectively by

$$\sigma_x^2 = (\sigma^* c)^2 \, \Gamma_{xx} \tag{7.6}$$

$$\sigma_y^2 = (\sigma^* c)^2 \, \Gamma_{yy} \tag{7.7}$$

$$\sigma_z^2 = (\sigma^* c)^2 \, \Gamma_{zz} \tag{7.8}$$

Similarly the total mean-squared error σ^2, and the so-called "geometric dilution of precision" (GDOP) are given by

$$\sigma^2 = \sigma_x^2 + \sigma_y^2 + \sigma_z^2 = (\sigma^* c)^2 \, (\Gamma_{xx} + \Gamma_{yy} + \Gamma_{zz}) \tag{7.9}$$

and

$$\text{GDOP} = \frac{\sigma}{\sigma^* c} = (\Gamma_{xx} + \Gamma_{yy} + \Gamma_{zz})^{1/2} \, . \tag{7.10}$$

Equations (7.6) - (7.10) show that the elements of the Γ matrix in (7.2) possess a simple interpretation. Specifically, the elements can be interpreted as <u>error magnification factors</u>. For example, Equation (7.6) asserts that the mean-squared error in the X' direction equals the mean-squared ranging error magnified by Γ_{xx}. Similarly, (7.9) asserts that the total mean-squared error σ^2 equals the mean-squared ranging error magnified by the factor $(\Gamma_{xx} + \Gamma_{yy} + \Gamma_{zz})$. Accordingly, the matrix $\underline{\Gamma}$ henceforth is called the <u>error magnification matrix</u>.

VIII. THE INVERSE ERROR MAGNIFICATION MATRIX

To deduce useful properties of the various measures of positional error, it is necessary to relate the error magnification matrix $\underline{\Gamma}$ or some function of it to the beacon-subject geometry. The present section shows that the inverse of $\underline{\Gamma}$ possesses two extremely simple interpretations in terms of system geometry. It is these interpretations that lead to the conclusions summarized in Section II.

Thus let $\underline{L}$ denote $\underline{\Gamma}^{-1}$. That is, let

$$\underline{L} = \underline{F}' \, \underline{H}'(\underline{H} \, \underline{P}_n \, \underline{H}')^{-1} \, \underline{H} \, \underline{F} \tag{8.1}$$

In Appendix I it is shown that the matrix factor $\underline{H}'(\underline{H} \, \underline{P}_n \, \underline{H}')^{-1} \, \underline{H}$ can be calculated from the expression

$$\underline{H}'(\underline{H} \, \underline{P}_n \, \underline{H}')^{-1} \, \underline{H} = [\underline{I} - \underline{M} \, \underline{U}(\underline{U}' \, \underline{M} \, \underline{U})^{-1} \, \underline{U}'] \, \underline{M}[\underline{I} - \underline{U}(\underline{U}' \, \underline{M} \, \underline{U})^{-1} \, \underline{U}'\underline{M}] \tag{8.2}$$

where

$$\underline{M} = \underline{P}_n^{-1} \quad \text{and} \quad \underline{U}' = [\underbrace{-1,1,1\ldots1}_{N+1}] \tag{8.3}$$

Use of (8.2) in (8.1) shows that

$$\underline{L} = \underline{K}' \, \underline{M} \, \underline{K} \tag{8.4}$$

where

$$K = [\underline{I} - U(U'M \, U)^{-1} \, U' \, M] \, \underline{F} \tag{8.5}$$

Equation (8.5) can be developed as follows:

$$\underline{K} = \left\{ \underline{I} - \frac{1}{\sum_{j=0}^{N} m_j} \begin{bmatrix} 1 \\ 1 \\ 1 \\ . \\ . \\ 1 \end{bmatrix} [-m_0, m_1, m_2, \ldots m_N] \right\} \begin{bmatrix} 0 \\ \underline{i}_1 \\ \underline{i}_2 \\ . \\ . \\ \underline{i}_N \end{bmatrix}$$

$$= \begin{bmatrix} 0 + \bar{\underline{i}} \\ \underline{i}_1 - \bar{\underline{i}} \\ \underline{i}_2 - \bar{\underline{i}} \\ \vdots \\ \underline{i}_N - \bar{\underline{i}} \end{bmatrix} \tag{8.6}$$

where m_j denotes the typical diagonal element of $\underline{M}$, $\underline{i}_j$ denotes the jth unit vector in row format, and

$$\bar{\underline{i}} = \frac{1}{\left(\sum_{j=0}^{N} m_j \right)} \sum_{j=1}^{N} m_j \, \underline{i}_j \tag{8.7}$$

To interpret the matrix $\underline{L}$, assume that the following construction is carried out.

Construction of Beacon Images on Unit Sphere

i) Draw a sphere of unit radius with center at the subject position 0.

ii) Draw the vectors $\underline{i}_1, \underline{i}_2 \ldots \underline{i}_N$ from the point 0.

iii) Place a mass of value $m_0 = (\sigma^*)^2/\sigma_0^2$ at the point 0; place masses of value $m_j = (\sigma^*)^2/\sigma_j^2$ $(j=1,2,\ldots N)$ respectively at the points where the unit vectors $\underline{i}_1, \underline{i}_2, \ldots \underline{i}_N$ terminate in the sphere (see Figure 8.1)

The vector $\underline{\bar{i}}$ specified by (8.7) can be interpreted as pointing from the point 0 to the center of mass CM of the mass configuration as shown in Figure 8.1. Likewise, the vector difference $\underline{i}_j - \underline{\bar{i}}$ contained in the jth row $(j \geq 1)$ of the matrix $\underline{K}$ can be interpreted as a vector pointing from CM to the mass m_j. Thus if (X,Y,Z) denotes a Cartesian coordinate system centered at CM, and differing from the system (X',Y',Z') only by a translation, then the elements of the jth row $(j \geq 1)$ of $\underline{K}$ are simply the coordinates X_j, Y_j and Z_j of the point P_j in the system (X,Y,Z).

That is,

$$\underline{K} = \begin{bmatrix} -X_0 & -Y_0 & -Z_0 \\ X_1 & Y_1 & Z_1 \\ \cdot & \cdot & \cdot \\ \cdot & \cdot & \cdot \\ X_N & Y_N & Z_N \end{bmatrix} \tag{8.8}$$

where X_0, Y_0, Z_0 denote the coordinates of the point 0 in the system (X,Y,Z). The desired formulation of $\underline{L}$ follows directly from (8.4) and (8.8); namely

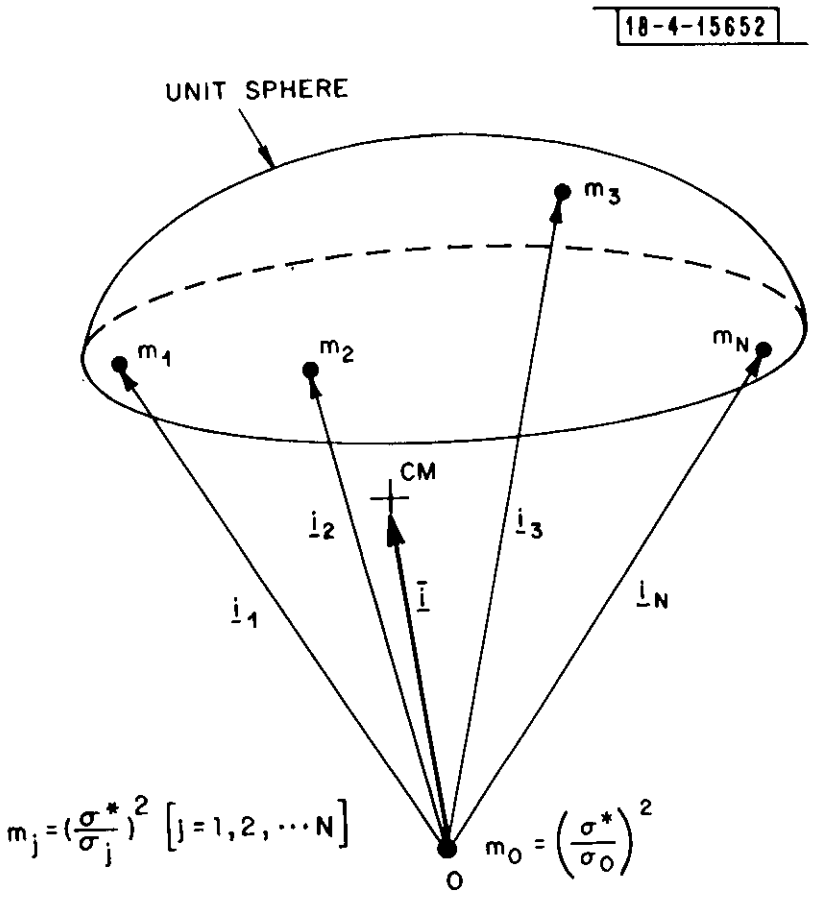
18-4-15652
UNIT SPHERE
m_3
m_1
m_2
m_N
CM
$\underline{i}_2$
$\underline{i}_3$
$\underline{\bar{i}}$
$\underline{i}_1$
$\underline{i}_N$
$m_j = (\frac{\sigma^*}{\sigma_j})^2 \; [j = 1, 2, \cdots N]$
$m_0 = \left(\frac{\sigma^*}{\sigma_0}\right)^2$
O

Figure 8.1

$$\underline{L} = \begin{bmatrix} \sum_{j=0}^{N} m_j X_j^2 & \sum_{j=0}^{N} m_j X_j Y_j & \sum_{j=0}^{N} m_j X_j Z_j \\ \sum_{j=0}^{N} m_j X_j Y_j & \sum_{j=0}^{N} m_j Y_j^2 & \sum_{j=0}^{N} m_j Y_j Z_j \\ \sum_{j=0}^{N} m_j X_j Z_j & \sum_{j=0}^{N} m_j Y_j Z_j & \sum_{j=0}^{N} m_j Z_j^2 \end{bmatrix} \tag{8.9}$$

where

$$m_j = \frac{(\sigma^*)^2}{(\sigma_j)^2} \tag{8.10}$$

In some cases it is useful to rewrite (8.9) as follows:

$$\underline{L} = M \times \begin{bmatrix} \frac{1}{M}\sum_{j=0}^{N} m_j X_j^2 & \frac{1}{M}\sum_{j=0}^{N} m_j X_j Y_j & \frac{1}{M}\sum_{j=0}^{N} m_j X_j Z_j \\ \frac{1}{M}\sum_{j=0}^{N} m_j X_j Y_j & \frac{1}{M}\sum_{j=0}^{N} m_j Y_j^2 & \frac{1}{M}\sum_{j=0}^{N} m_j Y_j Z_j \\ \frac{1}{M}\sum_{j=0}^{N} m_j X_j Z_j & \frac{1}{M}\sum_{j=0}^{N} m_j Y_j Z_j & \frac{1}{M}\sum_{j=0}^{N} m_j Z_j^2 \end{bmatrix}$$

where

$$M = \sum_{j=0}^{N} \frac{(\sigma^*)^2}{(\sigma_j)^2} \tag{8.12}$$

Equation (8.9) asserts that the entries in $\underline{L}$ are simply the moments and products of inertia of the mass configuration $m_0, m_1, m_2, .., m_N$ about its center of mass.

By contrast Equation (8.11) asserts that the entries in $\underline{L}$ can be regarded as averages of the second order products X^2, XY, XZ, etc. over the set of masses.

Both interpretations are highly useful.

IX. EXAMPLES

This section contains two examples which demonstrate the ease with which error measures can be calculated using the moment of inertia results of Section VIII. The examples utilize rather symmetrical geometries for the purpose of obtaining simple expressions for the error measures (7.6) - (7.10). As is evident from the derivation of Section VIII symmetry is not at all necessary to the method, however.

The examples are based upon two different beacon-subject geometries. One geometry is representative of satellite-based multilateration systems. The other geometry is representative of ground-based multilateration systems.

Example 9.1 (Satellite-Based Navigation)

Assume that an aircraft utilizes timing signals simultaneoulsy transmitted by four satellites to determine its position. Let the satellites be positioned at the corners and the center of an equilateral triangle at the time of signal transmission as shown in Figure 9.1.

Assume that the errors in the nominal satellite positions, the actual TOA errors at the aircraft, and the TOA measurement errors in the receiver correspond to an aggregate rms ranging error of $(\sigma_t c)$ feet for each signal path. Also assume that the error in the nominal time of signal transmission, the residual ionospheric delay, and the aircraft clock error correspond to an equivalent "clock error" having the rms value of σ_0 seconds.

The appropriate mass constellation takes the form shown in Figure 9.2. The masses m_1 - m_4 account for the ranging errors. The masses have unit value since, according to (7.3),

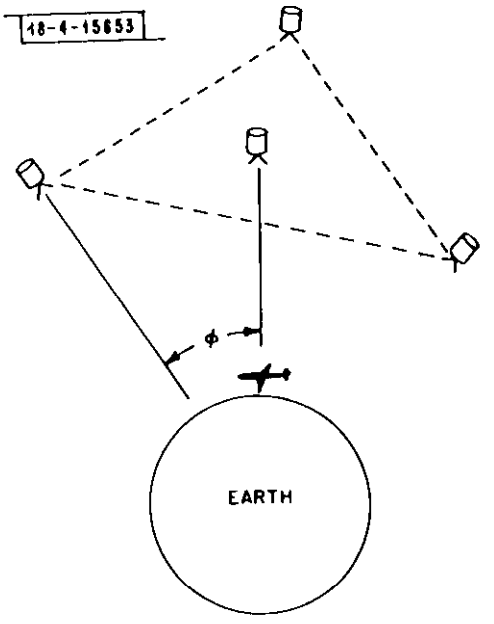

Figure 9.1

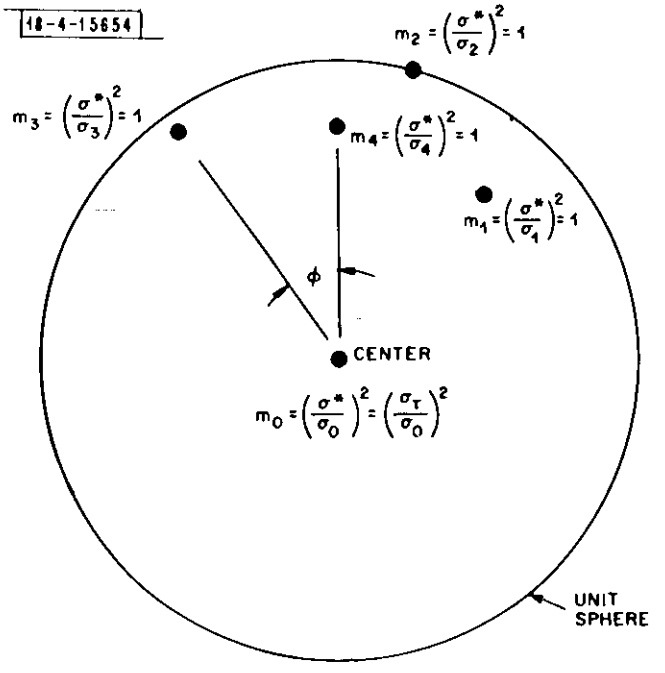

Figure 9.2

$$(\sigma^*)^2 = \frac{1}{4c^2} \sum_{j=1}^{4} (\sigma_t c)^2$$

$$= (\sigma_t)^2 \qquad (9.1)$$

and

$$m_j = \frac{(\sigma^*)^2}{(\sigma_j)^2} = \frac{(\sigma_t)^2}{(\sigma_t)^2} = 1 \qquad j = 1,2,3,4 \qquad (9.2)$$

The mass m_0 at the center of the sphere accounts for the clock error σ_0. The mass has the value

$$m_0 = (\sigma^*/\sigma_0)^2 = (\sigma_t/\sigma_0)^2 \qquad (9.3)$$

A simple calculation shows that the center of mass (CM) is located on the tetrahedral axis a distance

$$d = \frac{1 + 3\cos\phi}{4 + (\sigma_t/\sigma_0)^2} \qquad (9.4)$$

above m_0. Let (X,Y,Z) denote a Cartesian coordinate system at CM as indicated in Figure 9.3. Let (X_j, Y_j, Z_j) denote the coordinates of mass m_j with respect to CM. The elements of the $\underline{L}$ matrix (8.9) can be calculated straightforwardly as follows:

$$L_{xx} = m_1(\sin\phi)^2 + (m_2 + m_3)\left(\frac{1}{2}\sin\phi\right)^2$$

$$= \frac{3}{2}\sin^2\phi \qquad (9.5)$$

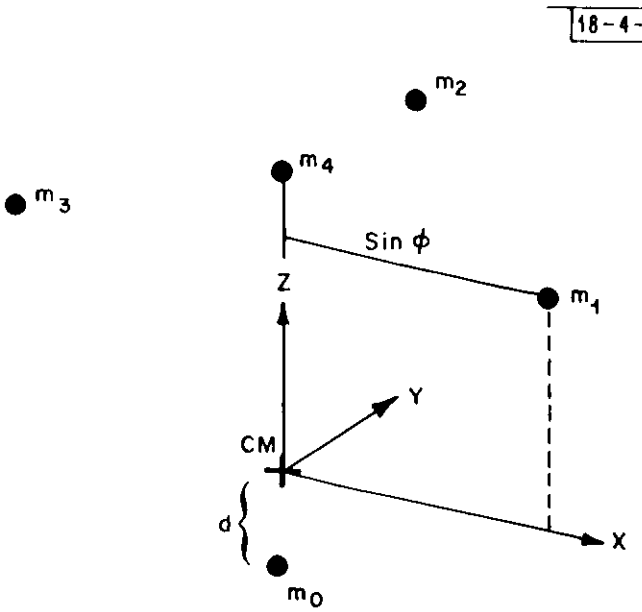

Figure 9.3

$$L_{yy} = (m_2 + m_3)\left(\frac{\sqrt{3}}{2}\sin\phi\right)^2$$

$$= \frac{3}{2}\sin^2\phi \tag{9.6}$$

$$L_{zz} = m_0 d^2 + (m_1 + m_2 + m_3)(\cos\phi - d)^2 + m_4(1 - d)^2$$

$$= \left[\frac{1}{\alpha + 1}(3\cos^2\phi + 1) + \frac{\alpha}{\alpha + 1}\frac{3}{4}(1 - \cos\phi)^2\right] \tag{9.7}$$

$$L_{xy} = L_{xz} = L_{yz} = 0 \tag{9.8}$$

where

$$\alpha \triangleq 4(\sigma_0/\sigma_t)^2 \tag{9.9}$$

Thus the $\underline{L}$ matrix is as follows:

$$\underline{L} = \begin{bmatrix} \frac{3}{2}\sin^2\phi & 0 & 0 \\ 0 & \frac{3}{2}\sin^2\phi & 0 \\ 0 & 0 & \dfrac{(3\cos^2\phi + 1) + \alpha\frac{3}{4}(1 - \cos\phi)^2}{(\alpha + 1)} \end{bmatrix} \tag{9.10}$$

The corresponding $\underline{\Gamma}$ matrix is given by

$$\underline{\Gamma} = \begin{bmatrix} \frac{2}{3}\frac{1}{\sin^2\phi} & 0 & 0 \\ 0 & \frac{2}{3}\frac{1}{\sin^2\phi} & 0 \\ 0 & 0 & \frac{\alpha + 1}{(3\cos^2\phi + 1) + \alpha\frac{3}{4}(1 - \cos\phi)^2} \end{bmatrix} \tag{9.11}$$

The expressions for the rms error magnification factors are as follows:

$$(\Gamma_{xx})^{1/2} = \sqrt{\frac{2}{3}}\ \frac{1}{\sin\phi} \tag{9.12}$$

$$(\Gamma_{yy})^{1/2} = \sqrt{\frac{2}{3}}\ \frac{1}{\sin\phi} \tag{9.13}$$

$$(\Gamma_{zz})^{1/2} = \sqrt{\frac{\alpha + 1}{(3\cos^2\phi + 1) + \alpha\frac{3}{4}(1 - \cos\phi)^2}} \tag{9.14}$$

$$\text{GDOP} = \sqrt{\frac{4}{3}\frac{1}{\sin^2\phi} + \frac{\alpha + 1}{(3\cos^2\phi + 1) + \alpha\frac{3}{4}(1 - \cos\phi)^2}} \tag{9.15}$$

For the values $\phi = 45°$, $\sigma_t = 30$ nsec, $\sigma_0 = 10$ nsec, the rms positional errors are

$$\sigma_x = \sigma_y = (\Gamma_{xx})^{1/2}\ (\sigma_t c) = 34.6 \text{ ft} \tag{9.16}$$

$$\sigma_z = (\Gamma_{zz})^{1/2}\ (\sigma_t c) = 22.7 \text{ ft} \tag{9.17}$$

$$\sigma = \text{GDOP} \times\ (\sigma_t c) = 53.9 \text{ ft} \tag{9.18}$$

If the clock error σ_0 is increased to 100 nsec the rms errors increase to

$$\sigma_x = \sigma_y = 34.6 \text{ ft} \tag{9.19}$$

$$\sigma_z = 87 \text{ ft} \tag{9.20}$$

$$\sigma = 100 \text{ ft} \tag{9.21}$$

END OF EXAMPLE

Example 9.2 (Ground-Based Surveillance)

Assume that round trip times from four ground based beacons are utilized to determine the position of an aircraft. Let the beacons be located at the corners and center of a very large equilateral triangle as shown in Figure 9.4. Let the aircraft be located near the center of the triangle at an elevation angle of 45° from the central beacon as shown.

Assume that the errors in the nominal beacon positions, anomalies in the round trip transit times and TOA measurement errors are equivalent to a one way ranging error of $(\sigma_t c)$ ft for each signal path. Assume also that the aircraft transponder imposes a residual delay on all signals equivalent to a one way rms clock error of σ_0 sec.

The mass constellation for this case is shown in Figure 9.5. The masses m_1 - m_4 account for the ranging error $(\sigma_t c)$. Again, the masses have unit value since

$$(\sigma^*)^2 = \frac{1}{4c^2} \sum_{j=1}^{4} (\sigma_t c)^2 = (\sigma_t)^2 \tag{9.22}$$

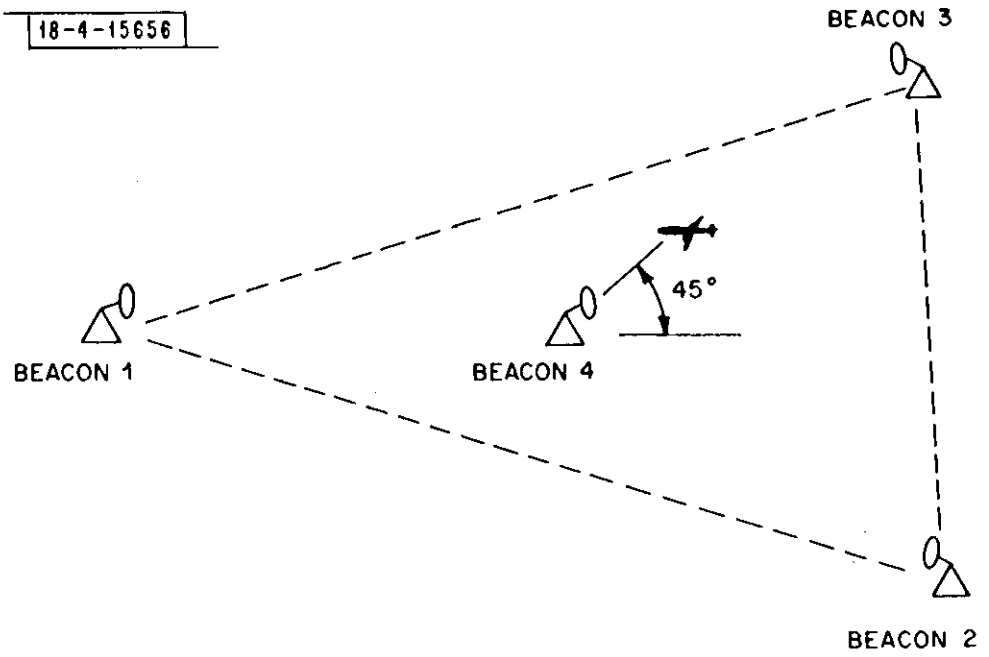

Figure 9.4

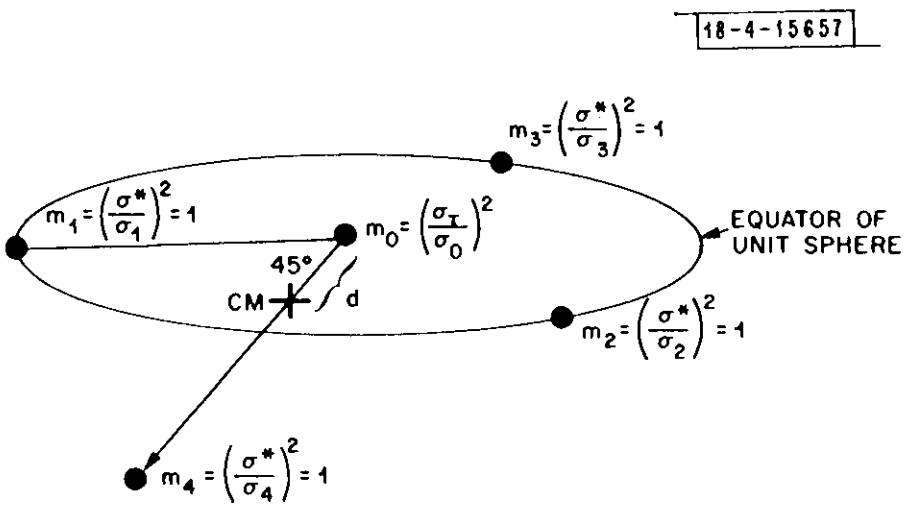

Figure 9.5

and

$$m_j = \frac{(\sigma^*)^2}{(\sigma_t)^2} = 1 \tag{9.23}$$

Masses m_1-m_3 are placed on the equator of the unit sphere since Beacons 1-3 are assumed to be on the aircraft's horizon. The mass m_0 at the center of the sphere accounts for the "clock error" σ_0.

The center of mass CM of the configuration is located a distance

$$d = m_4 \sum_{j=0}^{4} m_j \tag{9.24}$$

from the center of the sphere along the unit vector pointing to m_4 as shown in Figure 9.5.

Let (X,Y,Z) denote a Cartesian coordinate system at the CM oriented so that mass m_1 lies in the X-Z plane as shown in Figure 9.6 .

Straightforward calculation shows that the moments and products of inertia about the center of mass are as follows:

$$L_{xx} = \left[\frac{1}{\alpha + 1}(2) + \frac{\alpha}{\alpha + 1}(1.875)\right] \tag{9.25}$$

$$L_{yy} = \left[\frac{1}{\alpha + 1}(1.5) + \frac{\alpha}{\alpha + 1}(1.5)\right] \tag{9.26}$$

$$L_{zz} = \left[\frac{1}{\alpha + 1}(0.5) + \frac{\alpha}{\alpha + 1}(0.375)\right] \tag{9.27}$$

$$L_{xy} = 0 \tag{9.28}$$

$$L_{xz} = \left[\frac{1}{\alpha + 1}(0.5) + \frac{\alpha}{\alpha + 1}(0.375)\right] \tag{9.29}$$

$$L_{yz} = 0 \tag{9.30}$$

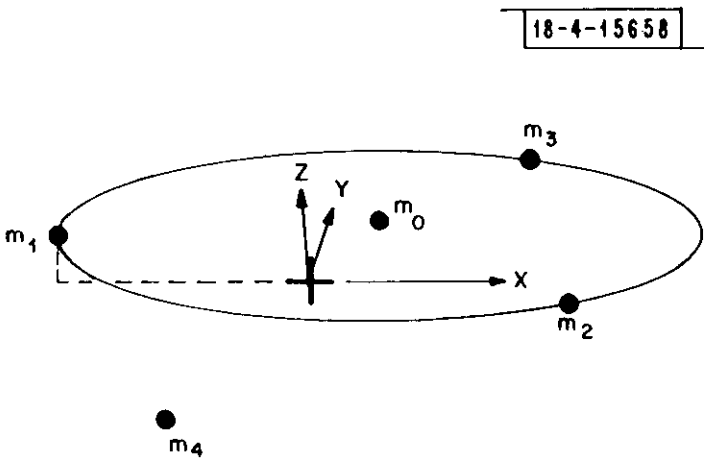

Figure 9.6

where

$$\alpha \triangleq \left(\sum_{j=1}^{4} m_j \right) / m_0 = 4(\sigma_0/\sigma_t)^2 \tag{9.31}$$

Consequently, the $\underline{L}$ matrix is

$$\underline{L} = \frac{1}{\alpha + 1} \begin{bmatrix} 2 & 0 & 0.5 \\ 0 & 1.5 & 0 \\ 0.5 & 0 & 0.5 \end{bmatrix} + \frac{\alpha}{\alpha + 1} \begin{bmatrix} 1.875 & 0 & 0.375 \\ 0 & 1.5 & 0 \\ 0.375 & 0 & 0.375 \end{bmatrix} \tag{9.32}$$

For the specific clock error $\sigma_0 = \sigma_t$ (or $\alpha = 4$), the corresponding $\underline{\Gamma}$ matrix is as follows:

$$\underline{\Gamma} = \begin{bmatrix} 0.667 & 0 & -0.667 \\ 0 & 0.667 & 0 \\ -0.667 & 0 & 3.166 \end{bmatrix} \tag{9.33}$$

The rms error magnification factors are given by

$$(\Gamma_{xx})^{1/2} = (\Gamma_{yy})^{1/2} = 0.816 \tag{9.34}$$

$$(\Gamma_{zz})^{1/2} = 1.779 \tag{9.35}$$

$$\text{GDOP} = 2.121 \tag{9.36}$$

For the values $\sigma_0 = \sigma_t = 20$ nsec, the rms errors in calculated position are as follows:

$$\sigma_x = \sigma_y = (\Gamma_{xx})^{1/2}(\sigma_t c) = 16.32 \text{ ft} \tag{9.37}$$

$$\sigma_z = (\Gamma_{zz})^{1/2}(\sigma_t c) = 37.58 \text{ ft} \tag{9.38}$$

$$\sigma = (\text{GDOP})\ (\sigma_t c) = 42.42 \text{ ft} \tag{9.39}$$

END OF EXAMPLE

X. THE LIMITING CASES $\sigma_0 \to 0$ AND $\sigma_0 \to \infty$

Obviously, as the rms clock error σ_0 decreases, the accuracy of a spherical multilateration system increases. Conversely, as the clock error σ_0 increases, accuracy decreases.

It is instructive to examine the mass configuration of Figure 8.1 to see how the foregoing conclusions derive from the moment of inertia viewpoint. The conclusions can be reached as follows. Decreasing σ_0 increases the mass m_0 at the origin. But increasing m_0 amounts to adding new mass to the system which must

1. Increase all moments of inertia and (thereby) increase the diagonal elements of the $\underline{L}$ matrix.
2. Correspondingly reduce the diagonal elements of the $\underline{r}$ matrix.

Thus the error magnification factors are reduced so that accuracy is increased. Conversely, increasing σ_0 amounts to removing mass from the system which produces the opposite effect.

Clearly, maximum accuracy is obtained as $\sigma_0 \to 0$. Here the center of mass has migrated to the center 0 of the unit sphere in Figure 8.1, so that the elements of $\underline{L}$ are moments and products of inertia taken about 0. Henceforth, this limiting form of a spherical system is called an ideal spherical system.

At the other extreme, minimum accuracy is obtained as the clock error $\sigma_0 \to \infty$. Here $m_0 = 0$ so that the moments are taken about the center of mass HCM of masses $m_1, m_2, \ldots m_N$. It has been shown elsewhere [9] that the $\underline{L}$ matrix calculated about HCM is the $\underline{L}$ matrix for a hyperbolic multilateration system having exactly the same beacon locations and ranging errors as the spherical system. Consequently, as $\sigma_0 \to \infty$ the accuracy of a spherical system degrades

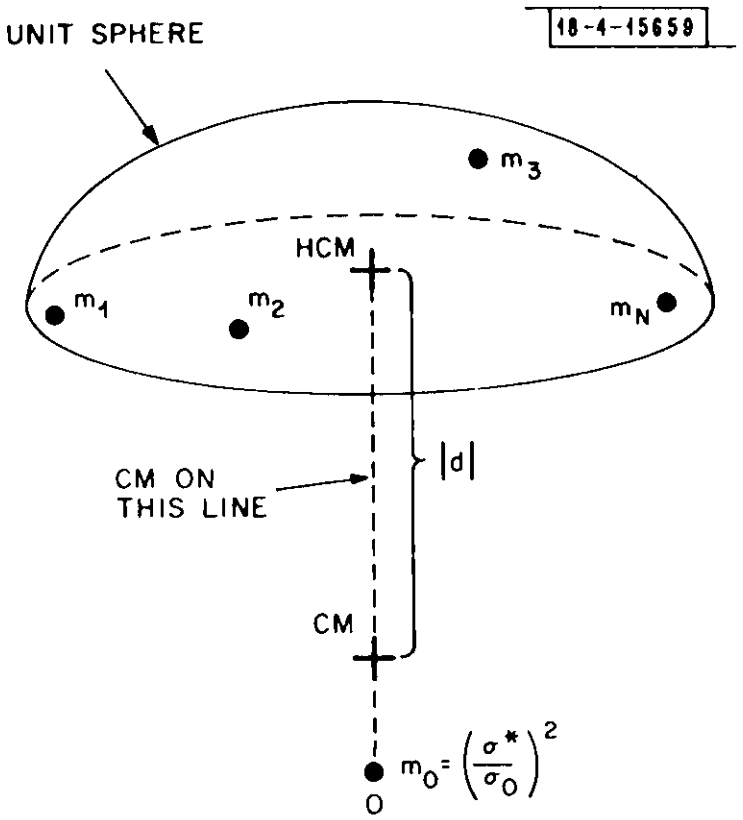
UNIT SPHERE
18-4-15659
m_3
HCM
m_1
m_2
m_N
|d|
CM ON
THIS LINE
CM
$m_0 = \left(\frac{\sigma^*}{\sigma_0}\right)^2$
0

Figure 10.1

to that of a comparable hyperbolic system.[1,2]

For values of σ_0 between zero and infinity the center of mass CM is located on a straight line connecting the points O and HCM as shown in Figure 10.1. The vector displacement $\underline{d}$ of the CM from HCM is given by

$$\underline{d} = \frac{1}{1 + \alpha} \underline{h} \tag{10.1}$$

where

$\underline{h}$ = a (3x1) vector pointing from O to HCM

$$\alpha = \left(\sum_{j=1}^{N} m_j \right) / m_0 \tag{10.2}$$

One might anticipate that for $|\underline{d}| \geq |\underline{h}|/2$, or equivalently,

$$m_0 \geq \sum_{j=1}^{N} m_j \tag{10.3}$$

that performance approximates that of an ideal spherical system, while for

$$m_0 < \sum_{j=1}^{N} m_j \tag{10.4}$$

[1]This conclusion agrees well with intuition. For assume that the same clock is used to record all TOAs. Clearly, as the clock error becomes large, the recorded TOAs lose their meaning; only the relative TOAs or TOA differences then contain useful information. Thus the accuracy of the spherical system must become identical to that of a comparable hyperbolic system.

[2]For a specific example, compare the limiting value of (9.15) with the result of Example 9.1 in Reference [1].

performance begins to degrade toward that of a hyperbolic system. For the special case

$$\sigma_1 = \sigma_2 = \ldots = \sigma_N = \boxed{\sigma_t} \tag{10.5}$$

condition (10.3) is equivalent to

$$1 \geq \frac{\sigma_0}{\sigma_t/\sqrt{N}} \tag{10.6}$$

Inequality (10.6) is discussed further in Sections XV and XVIII.

Equation (10.1) and the "parallel axis theorem" of elementary mechanics can be used to put the moment of inertia matrix in a particularly interesting form. Specifically, the parallel axis theorem states that

$$(\underline{L})_S = (\underline{L})_H + \left(\sum_{j=1}^{N} m_j\right) \underline{d}\,\underline{d}' + m_0(\underline{d} - \underline{h})(\underline{d} - \underline{h})'$$

$$= (\underline{L})_H + \left(\sum_{j=1}^{N} m_j\right) \frac{1}{1+\alpha}\,\underline{d}\,\underline{d}' \tag{10.7}$$

where

$(\underline{L})_S$ = The $\underline{L}$ matrix with moments taken about CM (i.e., the $\underline{L}$ matrix for the spherical system).

$(\underline{L})_H$ = The $\underline{L}$ matrix with moments taken about HCM (i.e., the $\underline{L}$ matrix for the hyperbolic system).

According to the previous discussion, the $\underline{L}$ matrix $(\underline{L})_0$ for an ideal spherical system is given by

$$(\underline{L})_0 = \lim_{\sigma_0 \to 0} [(\underline{L})_s]$$

$$= \lim_{m_0 \to \infty} [(\underline{L})_s]$$

$$= (\underline{L})_H + \left(\sum_{j=1}^{N} m_j \right) \underline{d}\, \underline{d}' \qquad (10.8)$$

Use of (10.8) to eliminate the product $\underline{d}\, \underline{d}'$ in (10.7) shows that

$$(\underline{L})_s = \frac{1}{1+\alpha} (\underline{L})_0 + \frac{\alpha}{1+\alpha} (\underline{L})_H \qquad (10.9)$$

Thus the $\underline{L}$ matrix for a spherical system is an interpolation between the $\underline{L}$ matrices for comparable ideal spherical and hyperbolic systems.[1]

A somewhat more complex argument shows that the $\underline{\Gamma}$ matrix for a spherical system likewise is a simple interpolation between the $\underline{\Gamma}$ matrix for a comparable ideal-spherical system and that for a comparable hyperbolic system. The result is

$$(\underline{\Gamma})_s = \frac{1}{1+\beta} (\underline{\Gamma})_0 + \frac{\beta}{1+\beta} (\underline{\Gamma})_H \qquad (10.10)$$

where

$$\beta = \frac{\alpha}{\left(\sum_{j=1}^{N} m_j \right) \underline{h}' (\underline{\Gamma})_H \underline{h} + 1} \qquad (10.11)$$

Equation (10.10) can be used to "prove" the conclusions on accuracy stated at the outset of the section. Specifically, the inequalities given on the following page are immediate consequences of (10.10)

[1] See Eq. (9.32) for a specific example.

$$(\Gamma_{xx})_0 \leq (\Gamma_{xx})_s \leq (\Gamma_{xx})_H \quad , \quad (\Gamma_{yy})_0 \leq (\Gamma_{yy})_s \leq (\Gamma_{yy})_H \qquad (10.12,13)$$

$$(\Gamma_{zz})_0 \leq (\Gamma_{zz})_s \leq (\Gamma_{zz})_H \quad , \quad (GDOP)_0 \leq (GDOP)_s \leq (GDOP)_H \qquad (10.14,15)$$

where the notations $(\ )_0$, $(\ )_s$ and $(\ )_H$ mean the indicated quantities evaluated for comparable ideal-spherical, spherical and hyperbolic systems.

XI. CALCULATION OF AVERAGE ERROR MEASURES

The error measures (7.6) - (7.10) for any specific beacon-subject geometry can be determined straightforwardly as indicated in Section IX. Accordingly, calculation of error measures for specific geometries is not discussed further.

In the next seven sections, the report develops general properties of spherical multilateration systems for the following cases of special interest.

Case I (Satellite-Based Systems):

The beacon images are confined to a viewing cone of half angle ϕ as indicated in Figure 11.1. Moreover, the rms ranging errors for all signal paths are equal.

Case II (Ground-Based Systems):

The beacon images are confined to a cone-complement of half angle ϕ as indicated in Figure 11.2. Again, the rms ranging errors for all signal paths are equal.

Case I includes most practical beacon constellations for satellite based systems. Case II includes most practical beacon constellations in which the beacons are far removed from the subject (aircraft). Applications in which one or more beacons are in the near vicinity of the subject can be analyzed by the method of Example 9.2.

An averaging procedure is used to develop the properties of such systems. The basic approach is as follows:

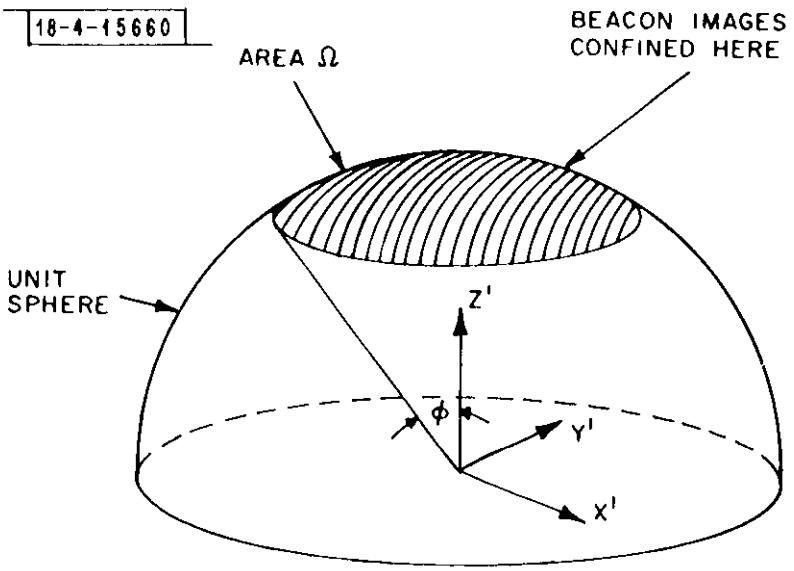

Figure 11.1

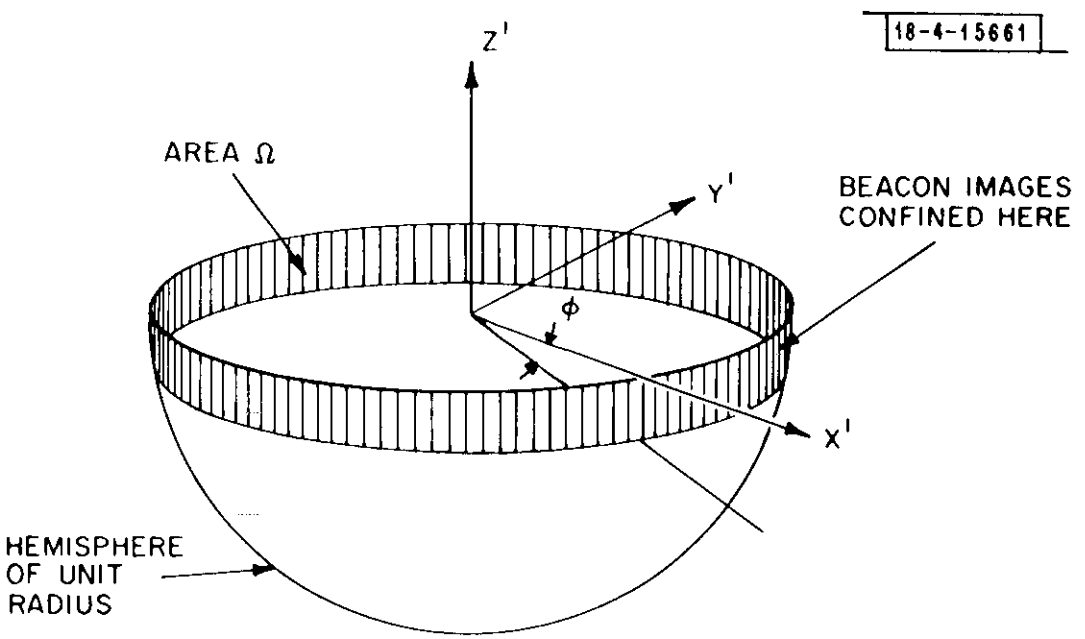

Figure 11.2

1. It is assumed that the image of each beacon can occupy any position within the allowed area Ω of the unit sphere; moreover, the beacon image positions are independent of each other, and all positions within Ω are equally likely.

2. The $\underline{L}$ matrix is averaged over all combinations of beacon image positions to obtain an average $\underline{L}$ matrix.

3. The average $\underline{L}$ matrix is inverted to obtain an (approximate) average $\underline{\Gamma}$ matrix.

4. Average error measures are extracted from the $\underline{\Gamma}$ matrix.

5. Properties are deduced from the resulting error measures.

This procedure leads much more directly to the basic properties of spherical systems than a detailed examination of typical cases.

The law of large numbers can be used to show that for large N the resulting "average" error measures are rigorous averages* in spite of the approximation

$$E[\underline{L}^{-1}] \approx (E[\underline{L}])^{-1} \tag{11.1}$$

in Step 3. For small values of N the resulting "average" quantities are only approximate averages.

In what follows the quantities produced by Steps 1 - 5 are simply called "average error measures." It is emphasized, however, that the averages are in fact approximate, with (11.1) being the approximation involved.

---

*Specifically if N is increased and σ_0^2 is decreased such that the quantity $\sum_{j=1}^{N} (\sigma_0/\sigma_j)^2$ remains constant, then the random matrix $N \times \underline{L}^{-1}$ converges to $N \times (E[\underline{L}])^{-1}$ with probability one as $N \to \infty$.

XII. THE AVERAGE $\underline{L}$ MATRIX

A general expression for the average $\underline{L}$ matrix is derived in Appendix II based upon the following assumptions.

A1. The masses $m_1, m_2, \ldots m_n$ are confined to a region Ω on the surface of the unit sphere.

A2. The mass positions within Ω are uncorrelated and are described by identical probability density functions.

The result specilized to the case

$$\sigma_1^2 = \sigma_2^2 = \ldots = \sigma_N^2 = \boxed{\sigma_t^2} \tag{12.1}$$

or equivalently

$$m_1 = m_2 = \ldots = m_N = \left(\frac{\sigma^*}{\sigma_t}\right)^2 = 1 \tag{12.2}$$

takes the following form

$$E[\underline{L}] = N\left[\frac{1}{1 + (N\,\sigma_0^2/\sigma_t^2)}\, E\left\{\begin{bmatrix} x' \\ y' \\ z' \end{bmatrix} [x' \quad y' \quad z']\right\}\right.$$

$$\left. + N\left(1 - \frac{1}{N}\right)\frac{N\sigma_0^2/\sigma_t^2}{1 + (N\,\sigma_0^2/\sigma_t^2)}\, E\left\{\begin{bmatrix} x' - \bar{x}' \\ y' - \bar{y}' \\ z' - \bar{z}' \end{bmatrix} [(x'-\bar{x}'),(y'-\bar{y}'),(z'-\bar{z}')]\right\}\right] \tag{12.3}$$

where E denotes expectation, and x',y',z' denote the coordinates (measured from the sphere center) of a random point P within Ω governed by the same probability density function as the masses $m_1, m_2, .., m_N$.

It is useful to rewrite (12.3) as follows to parallel (10.9)

$$E[\underline{L}] = \frac{1}{1+\alpha}\underline{L}_1 + \frac{\alpha}{1+\alpha}\underline{L}_2 \tag{12.4}$$

where

$$\alpha = N\,\sigma_0^2/\sigma_t^2 \tag{12.5}$$

$$\underline{L}_1 = N \times E\left\{\begin{bmatrix} x' \\ y' \\ z' \end{bmatrix} [x' \quad y' \quad z']\right\} \tag{12.6}$$

$$\underline{L}_2 = (1 - \tfrac{1}{N})\, N \times E\left\{\begin{bmatrix} x' - \bar{x}' \\ y' - \bar{y}' \\ z' - \bar{z}' \end{bmatrix} [(x'-\bar{x}'),(y'-\bar{y}'),(z'-\bar{z}')]\right\} \tag{12.7}$$

The formulation (12.4) asserts that the average $\underline{L}$ matrix is an interpolation of the matrices $\underline{L}_1$ and $\underline{L}_2$. The matrix $\underline{L}_1$ is the average $\underline{L}$ matrix for $m_0 = \infty$ (or $\sigma_0 = 0$), and therefore corresponds to the average $\underline{L}$ matrix for an ideal spherical system with beacon images confined to Ω. The matrix $\underline{L}_2$ is the average $\underline{L}$ matrix for $m_0 = 0$ (or $\sigma_0 = \infty$) and therefore corresponds to the average $\underline{L}$ matrix for a hyperbolic system with beacon images confined to Ω.

Note that the matrix $\underline{L}_2$ is disadvantaged compared to $\underline{L}_1$ by the factor $(1 - 1/N)$. This is due to the fact that for each sample mass configuration, the elements of $\underline{L}$ are moments about the sample CM rather than the mean CM. The disadvantage is most pronounced for $m_0 = 0$, or $E[\underline{L}] = \underline{L}_2$, in which case sample CMs can deviate considerably from the mean CM. The effect disappears for $m_0 = \infty$ or $E[\underline{L}] = \underline{L}_1$ in which case all sample CM's coincide with the mean CM.

In physical terms, the matrix $\underline{L}_1$ corresponds to the moment of inertia matrix about the sphere center of a thin shell confined to Ω and having mass density $N\rho$ where ρ denotes the probability density function describing the random point P. Similarly, the matrix $\underline{L}_2/(1 - 1/N)$ corresponds to the moment of inertia matrix for the same shell taken about its center of mass. For the case of a uniform probability density function (i.e., ρ = const.) it is easy to show that $\underline{L}_1$ and $\underline{L}_2$ take the following special forms.

Case I (Satellite-Based System)

$$\underline{L}_1 = N \begin{bmatrix} \frac{(1-\cos\phi)(2+\cos\phi)}{6} & 0 & 0 \\ 0 & \frac{(1-\cos\phi)(2+\cos\phi)}{6} & 0 \\ 0 & 0 & \frac{1+\cos\phi+\cos^2\phi}{3} \end{bmatrix} \tag{12.8}$$

$$\underline{L}_2 = \left(1 - \frac{1}{N}\right) N \begin{bmatrix} \frac{(1-\cos\phi)(2+\cos\phi)}{6} & 0 & 0 \\ 0 & \frac{(1-\cos\phi)(2+\cos\phi)}{6} & 0 \\ 0 & 0 & \frac{(1-\cos\phi)^2}{12} \end{bmatrix} \tag{12.9}$$

Case II (Ground Based System)

$$\underline{L}_1 = N \begin{bmatrix} \frac{1}{2}(1 - \frac{\sin^2\phi}{3}) & 0 & 0 \\ 0 & \frac{1}{2}(1 - \frac{\sin^2\phi}{3}) & 0 \\ 0 & 0 & \frac{1}{3}\sin^2\phi \end{bmatrix} \qquad (12.10)$$

$$\underline{L}_2 = (1 - \frac{1}{N})\, N \begin{bmatrix} \frac{1}{2}(1 - \frac{\sin^2\phi}{3}) & 0 & 0 \\ 0 & \frac{1}{2}(1 - \frac{\sin^2\phi}{3}) & 0 \\ 0 & 0 & \frac{1}{12}\sin^2\phi \end{bmatrix} \qquad (12.11)$$

Note that the entries in (12.8), (12.9) and (12.10), (12.11) are consistent with conditions (10.12) - (10.15).

XIII. SATELLITE-BASED SYSTEMS ($\sigma_0 \to 0$)

For $\sigma_0 \to 0$ the satellite-based system becomes an ideal spherical system. The corresponding average rms error measures can be calculated from the inverse of (12.4) with $\sigma_0 = 0$, or equivalently from the inverse of (12.8).

The results are as follows

$$(\Gamma_{xx})^{1/2} = (\Gamma_{yy})^{1/2} = \frac{1}{\sqrt{N}} \left[\frac{6}{(1 - \cos\phi)\ (2 + \cos\phi)}\right]^{1/2} \tag{13.1}$$

$$(\Gamma_{zz})^{1/2} = \frac{1}{\sqrt{N}} \left[\frac{3}{1 + \cos\phi + \cos^2\phi}\right]^{1/2} \tag{13.2}$$

$$\text{GDOP} = \frac{1}{\sqrt{N}} \left[\frac{12}{(1 - \cos\phi)\ (2 + \cos\phi)} + \frac{3}{1 + \cos\phi + \cos^2\phi}\right]^{1/2} \tag{13.3}$$

A plot of the average GDOP versus ϕ is given in Figure 13.1. The dashed curve represents the minimum GDOP obtainable from N beacons confined to a cone of half angle ϕ.[1] Note that the "average" curve is well above the "minimum" curve and exhibits the same general ϕ dependance.

Examination of (13.1)-(13.3) shows that all error measures are proportional to $1/\sqrt{N}$. This means that the error measures are not highly sensitive to the number N of beacons. For example, to halve GDOP by the expedient of adding beacons, it is necessary to increase the number of beacons by a factor of four.

[1] The expression for minimum GDOP is derived in Section XX.

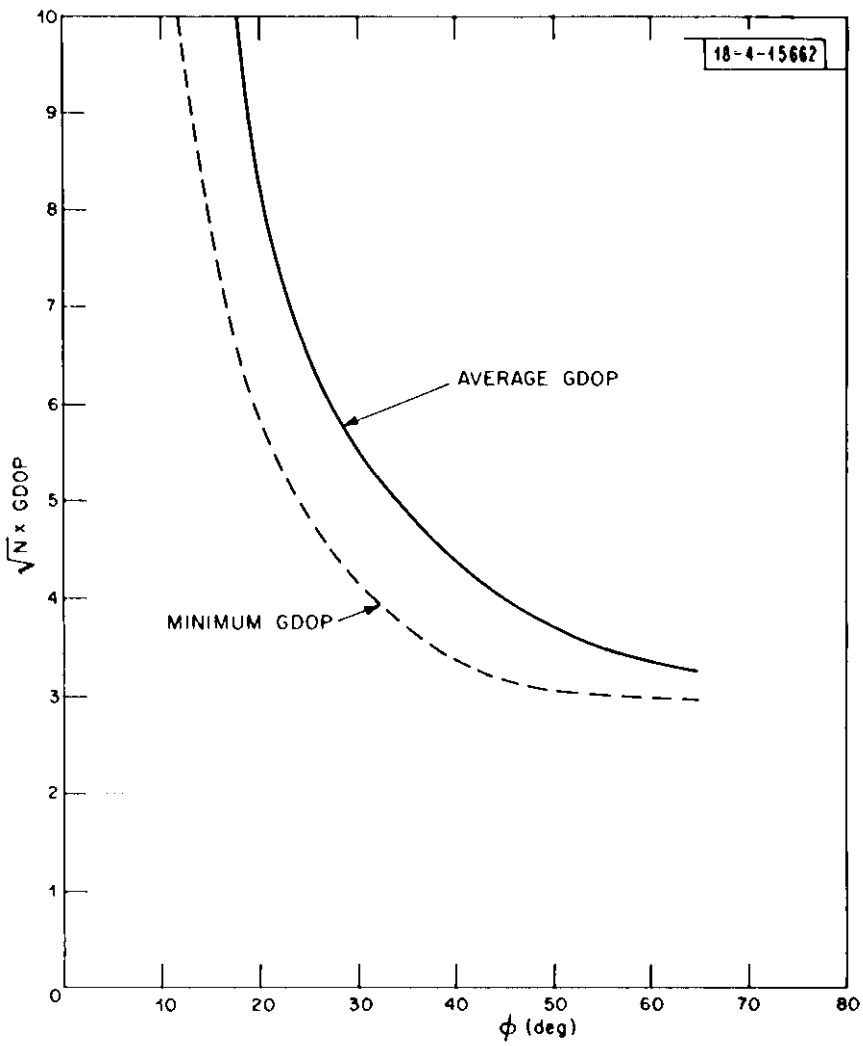
18-4-15662
AVERAGE GDOP
MINIMUM GDOP
$\sqrt{N}$ x GDOP
ϕ (deg)
0
1
2
3
4
5
6
7
8
9
10
10
20
30
40
50
60
70
80

Figure 13.1

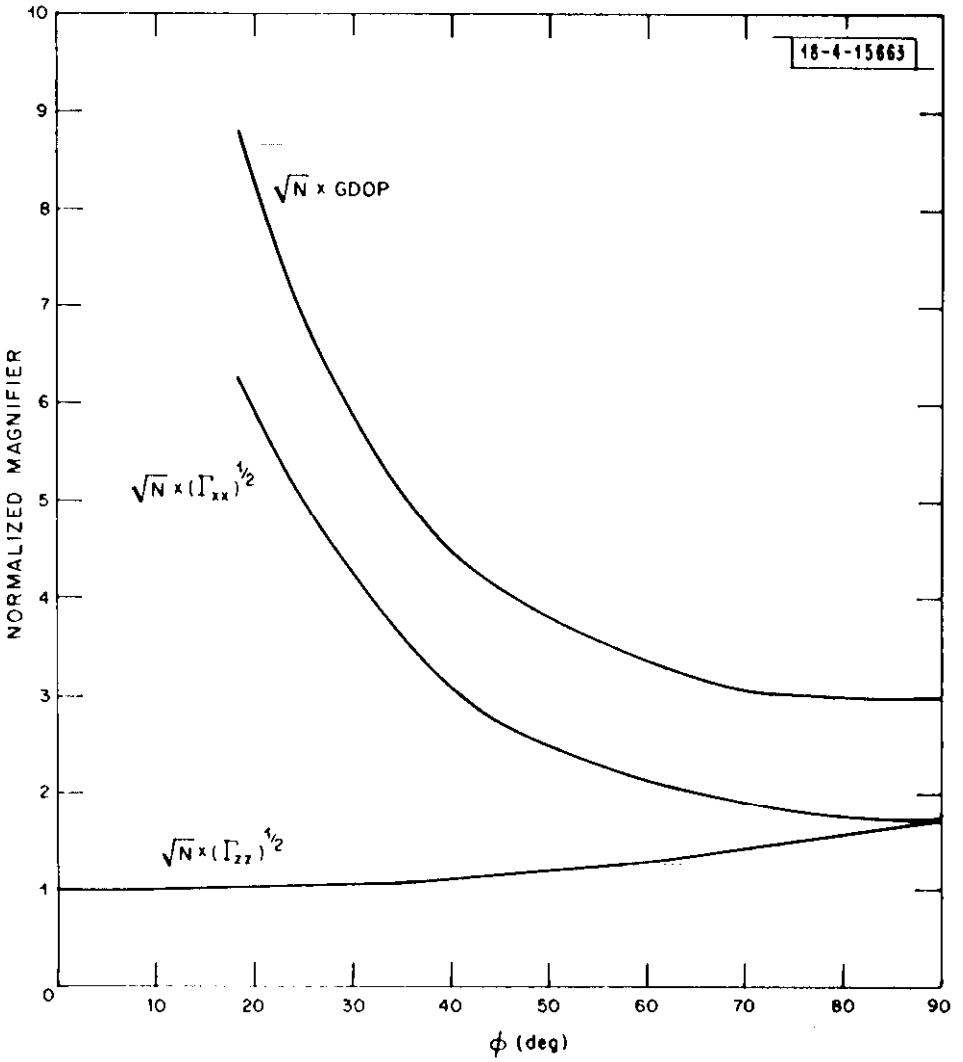
18-4-15663
NORMALIZED MAGNIFIER
$\sqrt{N}$ x GDOP
$\sqrt{N} \times (\Gamma_{xx})^{1/2}$
$\sqrt{N} \times (\Gamma_{zz})^{1/2}$
ϕ (deg)
0
1
2
3
4
5
6
7
8
9
10
10
20
30
40
50
60
70
80
90

Figure 13.2

Normalized plots of the rms error measures are given in Figure 13.2. The following conclusions are evident from the figure.

1. Accuracy is much more sensitive to cone angle than to N. For example, increasing ϕ from $\phi = 30^{\circ}$ to $\phi = 60^{\circ}$ halves GDOP, an improvement that otherwise would require a fourfold increase in the number of beacons.
2. Errors in position are primarily horizontal errors. For example, for $\phi = 45^{\circ}$, $(\Gamma_{xx})^{1/2} \approx 2(\Gamma_{zz})^{1/2}$ so that rms horizontal errors exceed rms vertical errors by a factor of two.

XIV. SATELLITE-BASED SYSTEMS ($\sigma_0 \to \infty$)

For $\sigma_0 \to \infty$ the satellite-based system degrades to a hyperbolic system. The corresponding average error measures can be found from the inverse of (12.4) with $\sigma_0 = \infty$, or equivalently from the inverse of (12.9).

The resulting error measures are as follows:

$$(\Gamma_{xx})^{1/2} = (\Gamma_{yy})^{1/2} = \frac{1}{\sqrt{N-1}} \left[\frac{6}{(1 - \cos\phi)(2 + \cos\phi)} \right]^{1/2} \tag{14.1}$$

$$(\Gamma_{xx})^{1/2} = \frac{1}{\sqrt{N-1}} \frac{2\ 3}{1 - \cos\phi} \tag{14.2}$$

$$\text{GDOP} = \frac{1}{\sqrt{N-1}} \left[\frac{12}{(1 - \cos\phi)(2 + \cos\phi)} + \frac{12}{(1 - \cos\phi)^2} \right]^{1/2} \tag{14.3}$$

Again, the error measures substantially have a $1/\sqrt{N}$ dependence so that accuracy is not highly sensitive to N.

Normalized plots of the error measures are shown in Figure 14.1 for $N = 4$ and $N = \infty$. The curves for $4 < N < \infty$ lie between the $N = 4$ and $N = \infty$ curves. The following conclusions can be drawn from the figure:[1]

1. Again accuracy is highly sensitive to cone angle. For example, increasing ϕ from 40° to 60° halves GDOP or double over-all accuracy.

2. Altitude accuracy is much poorer than horizontal accuracy. For example, at $\phi = 45°$ altitude errors typically exceed horizontal errors by a factor of three.

[1] The same conclusions are drawn in Reference [1] using different arguments.

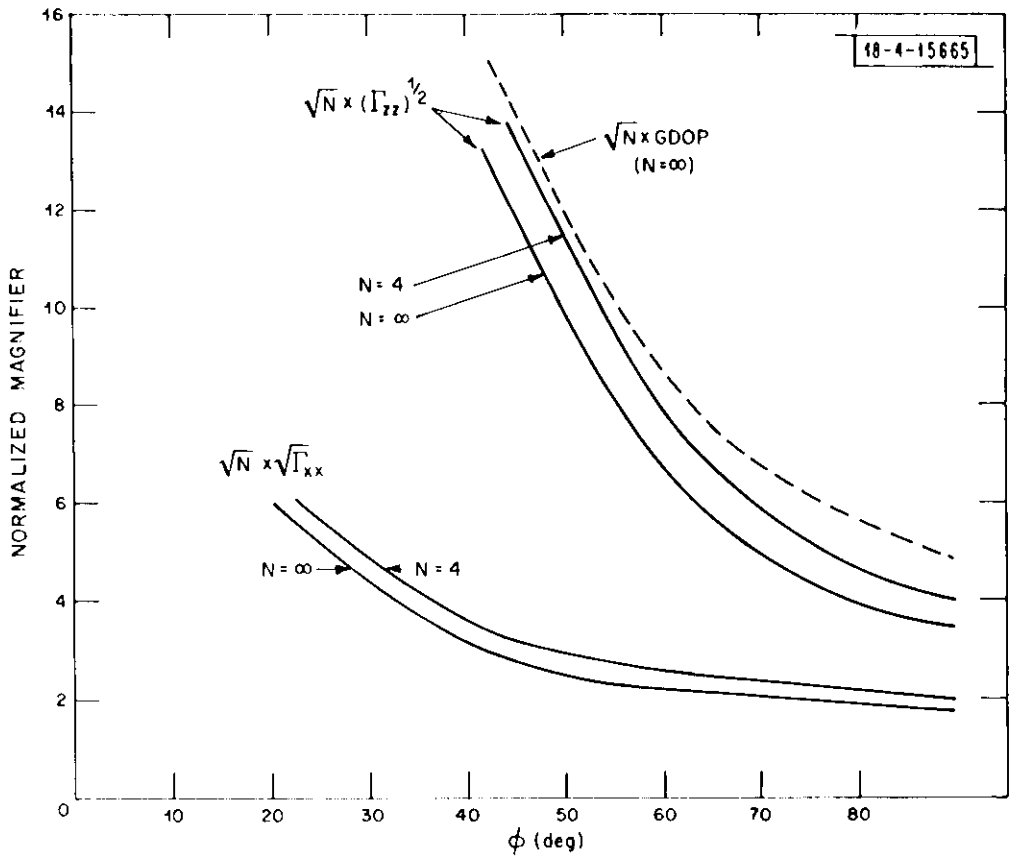
18-4-15665
NORMALIZED MAGNIFIER
$\sqrt{N} \times (\Gamma_{zz})^{1/2}$
$\sqrt{N} \times$ GDOP
(N=∞)
N = 4
N = ∞
$\sqrt{N} \times \sqrt{\Gamma_{xx}}$
N = ∞
N = 4
0
2
4
6
8
10
12
14
16
10
20
30
40
50
60
70
80
ϕ (deg)

Figure 14.1

Figures 14.2-14.4 contrast plots of the average rms error measures vs. ϕ for the limiting cases $\sigma_0 = 0$ (ideal spherical) and $\sigma_0 = \infty$ (hyperbolic). The following conclusions can be drawn from the curves.

Ideal-Spherical vs. Hyperbolic

1. Altitude accuracy is much better for the ideal spherical system. For example, Figure 14.2 shows that for $\phi = 45°$ altitude errors for the ideal spherical system typically are an order of magnitude smaller than those for the hyperbolic system.

2. The horizontal accuracies are comparable for the two limiting cases. Specifically, the plots of $(\Gamma_{xx})^{1/2}\sqrt{N}$ shown in Figure 14.3 are almost identical.

3. Over-All Accuracy (GDOP) is Signficantly Better for the Ideal Spherical system. For example, Figure 14.4 shows that for $\phi = 45^{o}$ GDOP for the ideal spherical system typically is one fourth of that for the hyperbolic system.

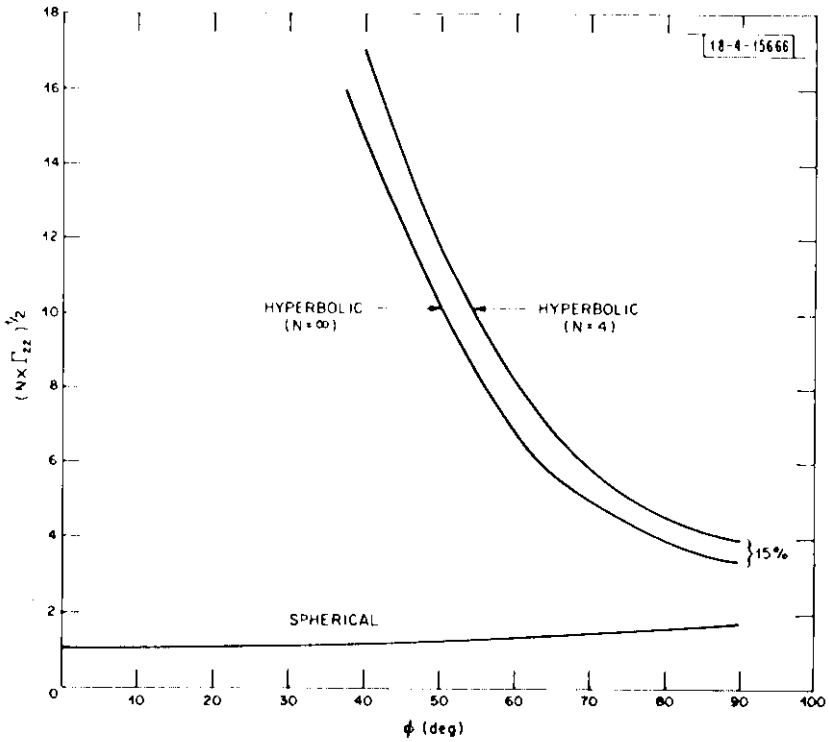

Figure 14.2

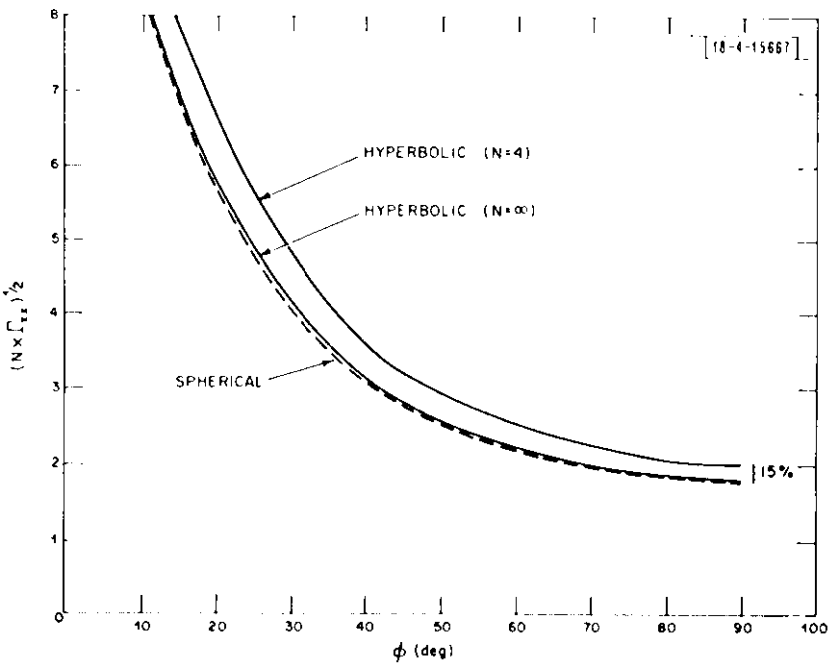

Figure 14.3

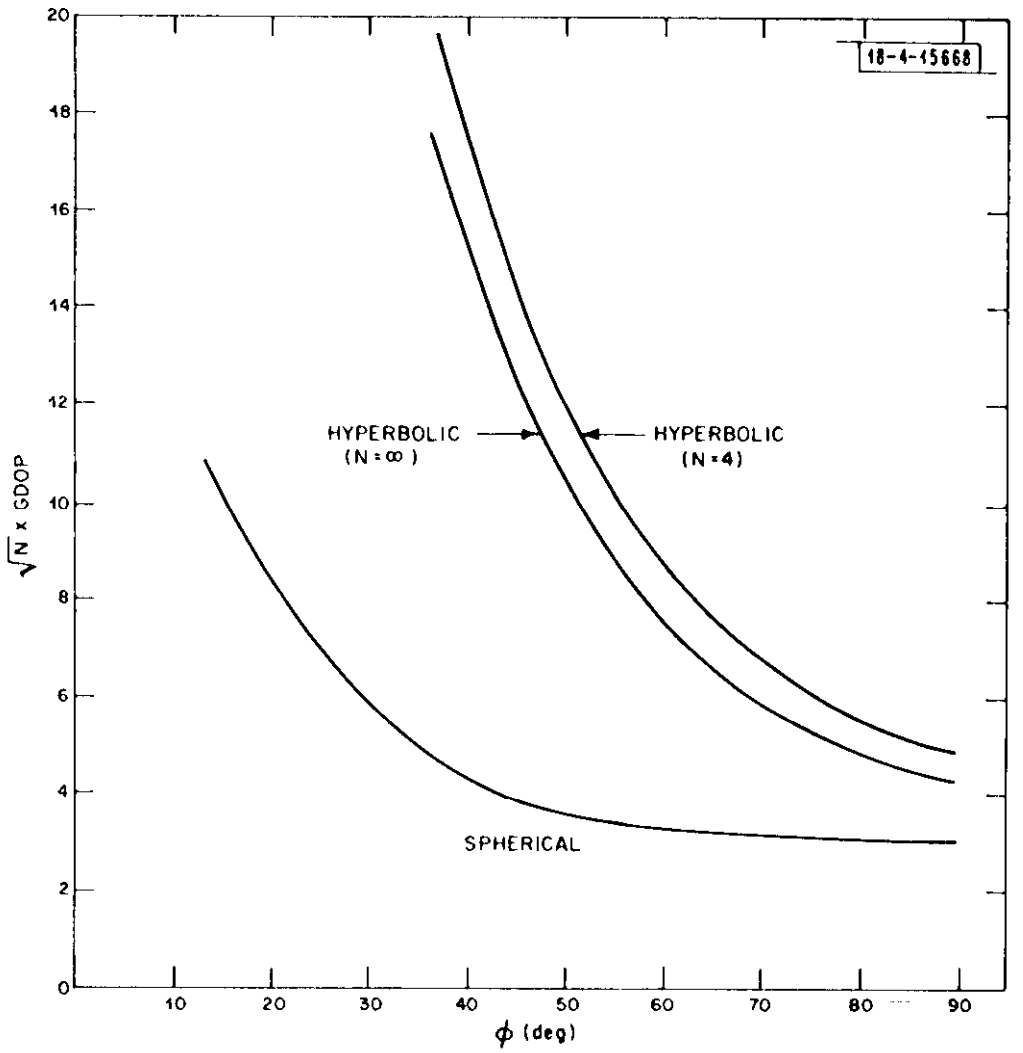
18-4-15668
HYPERBOLIC
(N = ∞)
HYPERBOLIC
(N = 4)
SPHERICAL
√N x GDOP
φ (deg)
0
2
4
6
8
10
12
14
16
18
20
10
20
30
40
50
60
70
80
90

Figure 14.4

XV. SATELLITE-BASED SYSTEMS (General Case)

The extent to which the benefits of a $\sigma_0 = 0$ (or ideal) spherical system are realized depends upon the size of the clock error σ_0 relative to the normalized ranging error[1] $\sigma_t/\sqrt{N}$.

Average rms error measures for different values of σ_0 can be calculated from the inverse of (12.4). Plots of the resulting error measures versus the normalized variable $\sqrt{N}\ \sigma_0/\sigma_t$ are shown in Figures 15.1-15.3.

It is clear from Figures 15.1-15.3 that accuracies typical of an ideal spherical system are obtained provided

$$\sigma_0 < \sigma_t/\sqrt{N} \tag{15.1}$$

As σ_0 is increased beyond $\sigma_t/\sqrt{N}$, accuracy degrades and approaches that typical of a hyperbolic system. Figure 15.1 shows that altitude accuracy degrades rapidly as σ_0 is increased beyond $\sigma_t/\sqrt{N}$ and substantially equals that of a hyperbolic system for $\sigma_0 > 50\ \sigma_t/\sqrt{N}$. Figure 15.2 shows that horizontal accuracy decreases only slightly as σ_0 exceeds $\sigma_t/\sqrt{N}$ and roughly equals that of a hyperbolic system for $\sigma_0 > 5\ \sigma_t/\sqrt{N}$. Total rms error or GDOP has a $\sqrt{N}\ \sigma_0/\sigma_t$ dependence similar to that of Γ_{zz}, which dominates the GDOP calculations for $\sigma_0 > 5\ \sigma_t/\sqrt{N}$.

The curves of Figures 15.1-15.3 are useful for assessing the effect of clock improvements. For example, it is clear that for $\sigma_0 < \sigma_t/\sqrt{N}$ clock improvements will not significantly improve accuracy. By contrast, for $\sigma_0 = 10\ \sigma_t/\sqrt{N}$ clock improvements substantially increase accuracy.[2]

---

[1] This is reasonable since in the absence of a clock input, accuracy is proportional to $\sigma_t/\sqrt{N}$. Thus for the clock to impact accuracy, σ_0 should be small compared to $\sigma_t/\sqrt{N}$ times a geometric factor. Also, see Section X.

[2] Note that actual clock error is only one component of the error σ_0 [see (5.3)]. Thus there is a limit to the reduction in σ_0 that can be achieved by improvements to the actual clock.

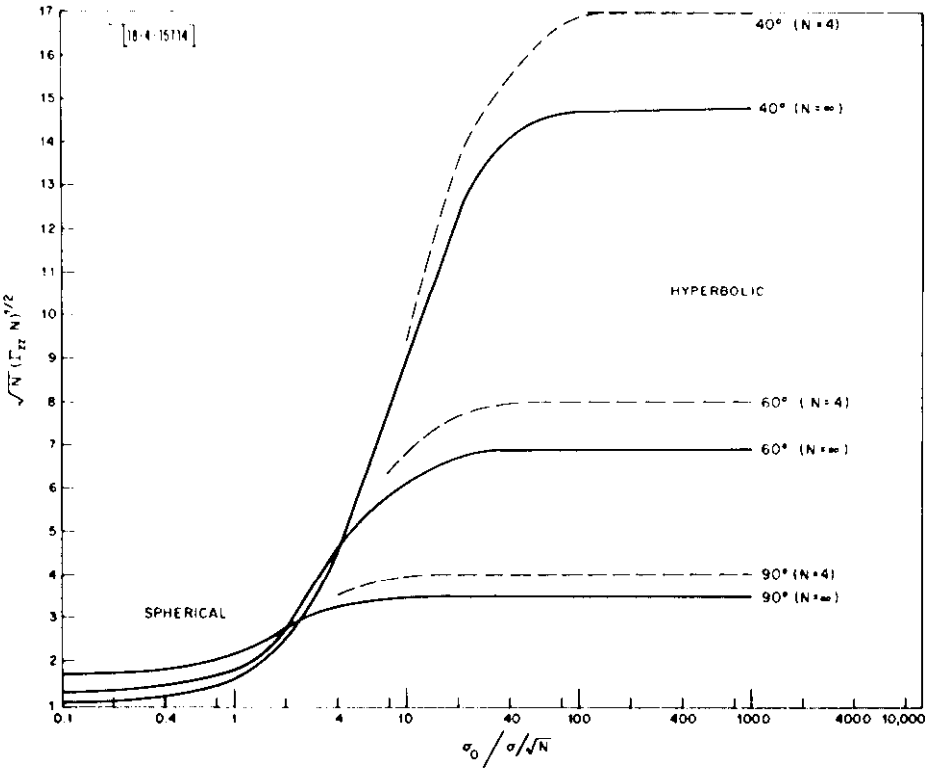

Figure 15.1

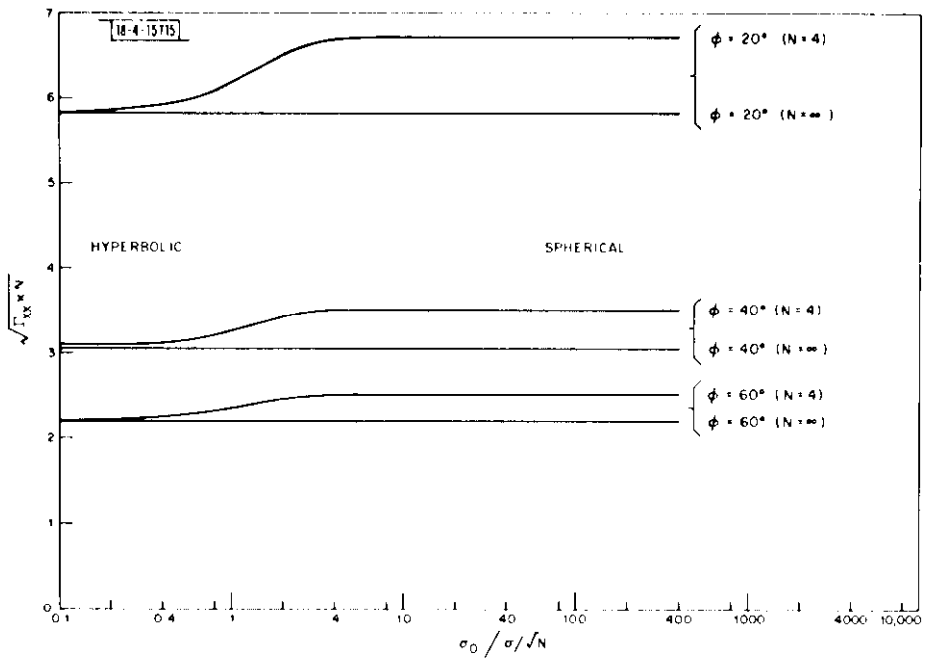

Figure 15.2

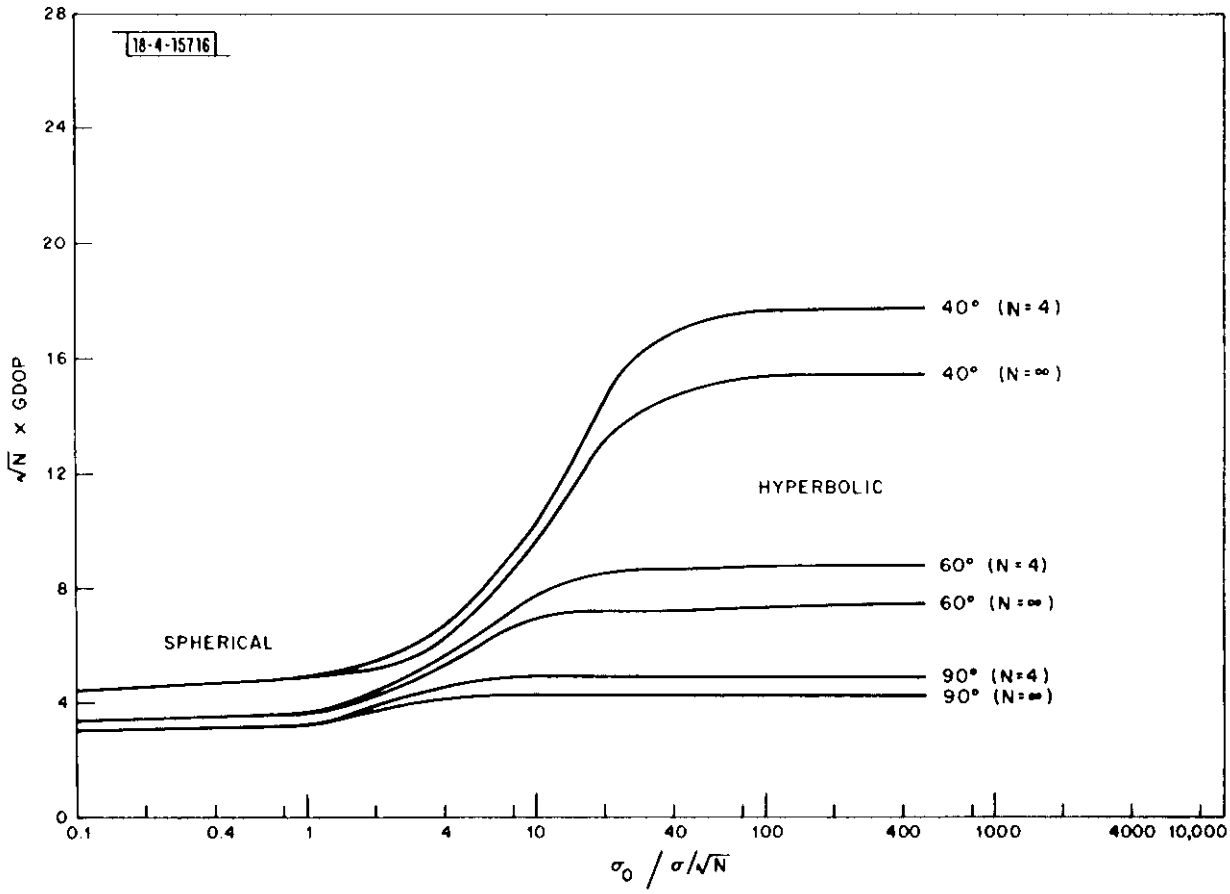
18-4-15716
28
24
20
16
12
8
4
0
$\sqrt{N}$ x GDOP
40° (N=4)
40° (N=∞)
HYPERBOLIC
60° (N=4)
60° (N=∞)
SPHERICAL
90° (N=4)
90° (N=∞)
0.1
0.4
1
4
10
40
100
400
1000
4000
10,000
$\sigma_0 / \sigma/\sqrt{N}$

Figure 15.3

XVI. GROUND-BASED SYSTEMS ($\sigma_0 \to 0$)

For $\sigma_0 \to 0$ the ground-based system becomes an ideal spherical system. The average rms error measures can be determined from the inverse of (12.10).

The results are as follows.

$$(\Gamma_{xx})^{1/2} = (\Gamma_{yy})^{1/2} = \frac{1}{\sqrt{N}} \left[\frac{2}{1 - \frac{\sin^2 \phi}{3}} \right]^{1/2} \tag{16.1}$$

$$(\Gamma_{zz})^{1/2} = \frac{1}{\sqrt{N}} \frac{\sqrt{3}}{\sin \phi} \tag{16.2}$$

$$\text{GDOP} = \frac{1}{\sqrt{N}} \left[\frac{4}{1 - \frac{\sin^2 \phi}{3}} + \frac{3}{\sin^2 \phi} \right]^{1/2} \tag{16.3}$$

Again the error measures have a $1/\sqrt{N}$ dependence. Consequently accuracy is not highly sensitive to the number N of beacons.

Normalized plots of the error measures $(\Gamma_{xx})^{1/2}$ and $(\Gamma_{zz})^{1/2}$ versus the maximum elevation angle ϕ are shown in Figure (16.1). The following conclusions are apparent from the figure.

1. Horizontal errors are comparatively small and independent of ϕ.
2. By contrast altitude errors are large and highly sensitive to ϕ. Indeed as $\phi \to 0$ altitude discrimination disappears altogether.

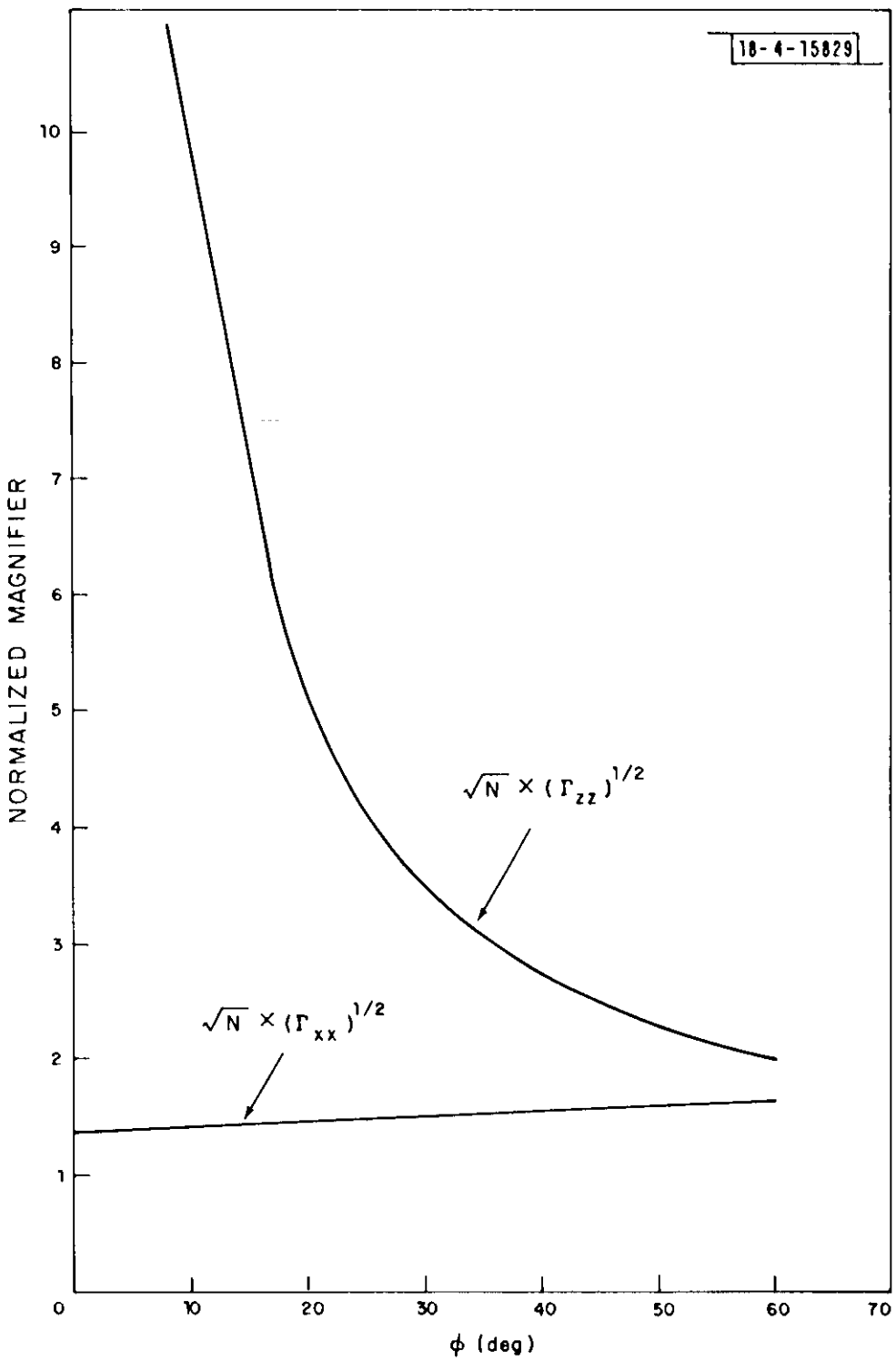
18-4-15829
NORMALIZED MAGNIFIER
$\sqrt{N} \times (\Gamma_{zz})^{1/2}$
$\sqrt{N} \times (\Gamma_{xx})^{1/2}$
ϕ (deg)
0
10
20
30
40
50
60
70
1
2
3
4
5
6
7
8
9
10

Figure 16.1

XVII. GROUND-BASED SYSTEMS ($\sigma_0 \to \infty$)

For $\sigma_0 \to \infty$ the ground-based system becomes a hyperbolic system. Thus the rms accuracy measures can be determined from the inverse of (12.11).

The results are as follows.

$$(\Gamma_{xx})^{1/2} = (\Gamma_{yy})^{1/2} = \frac{1}{\sqrt{N-1}} \left[\frac{2}{1 - \frac{\sin^2 \phi}{3}} \right]^{1/2} \tag{17.1}$$

$$(\Gamma_{zz})^{1/2} = \frac{1}{\sqrt{N-1}} \frac{2\sqrt{3}}{\sin \phi} \tag{17.2}$$

$$\text{GDOP} = \frac{1}{\sqrt{N-1}} \left[\frac{4}{1 - \frac{\sin^2 \phi}{3}} + \frac{12}{\sin^2 \phi} \right]^{1/2} . \tag{17.3}$$

As in all preceding cases, the error measures substantially have a $1/\sqrt{N}$ dependence. Thus accuracy is relatively insensitive to the number of beacons.

Normalized plots of $(\Gamma_{xx})^{1/2}$ and $(\Gamma_{zz})^{1/2}$ versus ϕ are shown in Figure 17.1. Once again

1. Horizontal errors are small and relatively independent of ϕ.
2. Altitude errors are large and very sensitive to ϕ.

Figures 17.2 and 17.3 compare normalized plots of $(\Gamma_{yx})^{1/2}$ and $(\Gamma_{zz})^{1/2}$ vs. ϕ for hyperbolic and ideal spherical systems. Figure 17.2 shows that

1. The horizontal accuracies of two systems are almost identical.

It is clear from Figure 17.3 that

2. While the altitude accuracy of both systems is poor, the altitude accuracy of the ideal spherical system is approximately twice as good as that of the hyperbolic system.

Thus the primary difference in performance of the limiting cases is in altitude descrimintation where the ideal spherical system performs approximately twice as well.

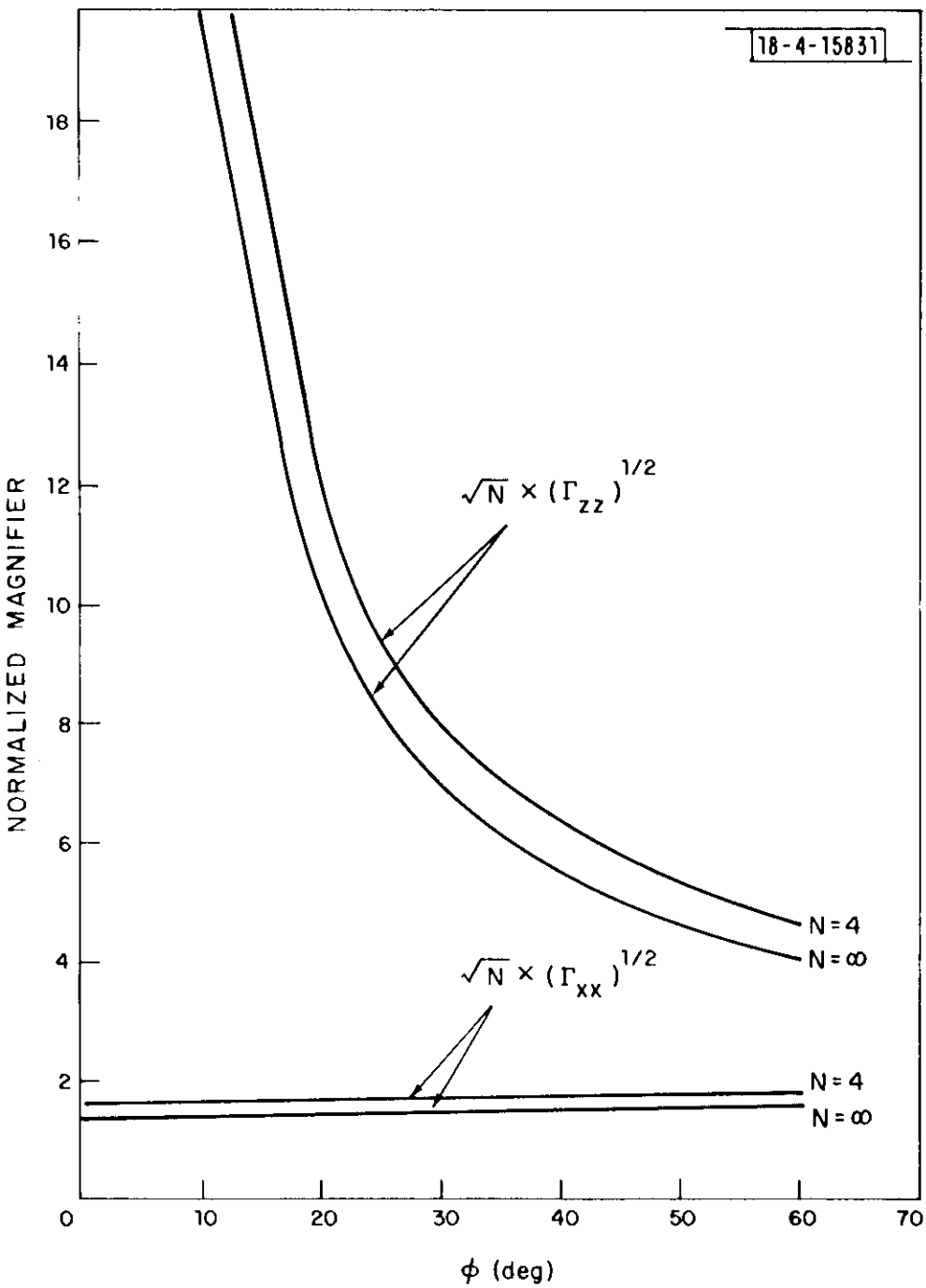
18-4-15831
NORMALIZED MAGNIFIER
18
16
14
12
10
8
6
4
2
0
10
20
30
40
50
60
70
ϕ (deg)
$\sqrt{N} \times (\Gamma_{zz})^{1/2}$
N = 4
N = ∞
$\sqrt{N} \times (\Gamma_{xx})^{1/2}$
N = 4
N = ∞

Figure 17.1

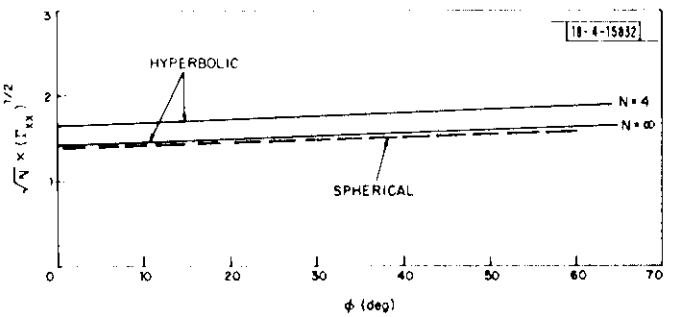

Figure 17.2

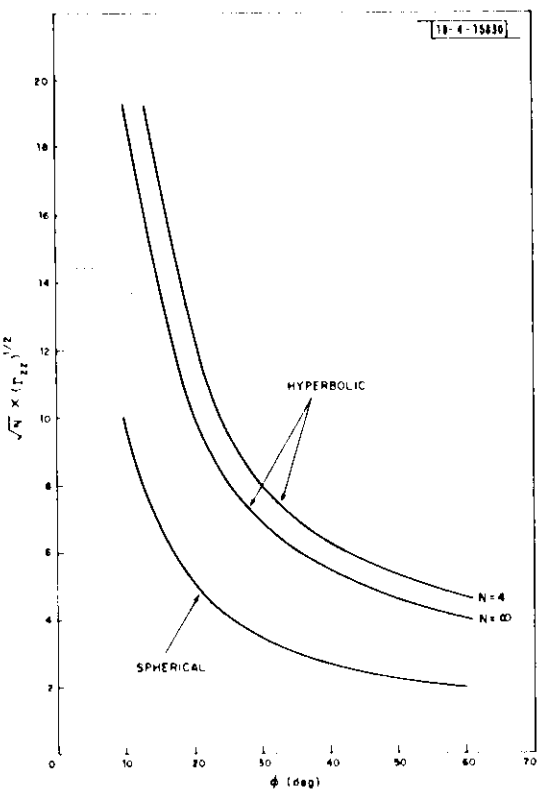

Figure 17.3

XVIII. GROUND-BASED SYSTEMS (General Case)

The extent to which a ground-based system achieves the better altitude discrimination of a pure spherical system depends upon the value of the rms clock error σ_0 relative to the normalized ranging error $\sigma_t/\sqrt{N}$.

The average rms error measures for different values of $\sigma_0/(\sigma_t/\sqrt{N})$ can be calculated from the inverse of (12.4) using (12.10) and (12.11).

Figures 18.1 and 18.2 show normalized plots of the error measures versus $\sqrt{N}\,\sigma_0/\sigma_t$. The curves start from the values for an ideal spherical system and degrade to those of a hyperbolic system as σ_0 becomes large. For $5° \leq \phi \leq 10°$ the error measures approximate those of an ideal spherical system provided

$$\sigma_0 < \sigma_t/\sqrt{N} \tag{18.1}$$

For $5° \leq \phi \leq 10°$ the error measures approximate those of a hyperbolic system whenever

$$\sigma_0 > 5\,\sigma_t/\sqrt{N} \tag{18.2}$$

Thus almost a factor of two improvement in altitude discrimination over a hyperbolic system is obtained whenever (18.1) is satisfied. No improvement is achieved when (18.2) is satisfied. A modest improvement is obtained for

$$\sigma_t/\sqrt{N} < \sigma_0 < 5\,\sigma_t/\sqrt{N} \tag{18.3}$$

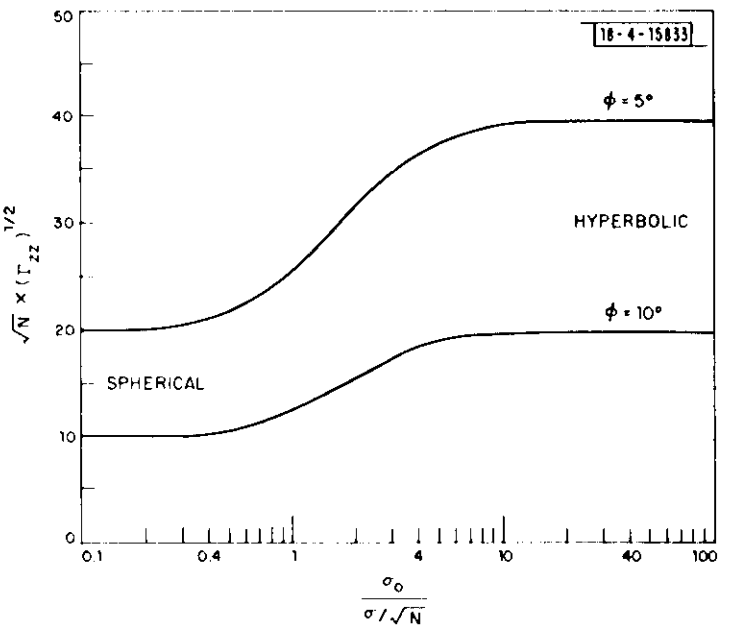

Figure 18.1

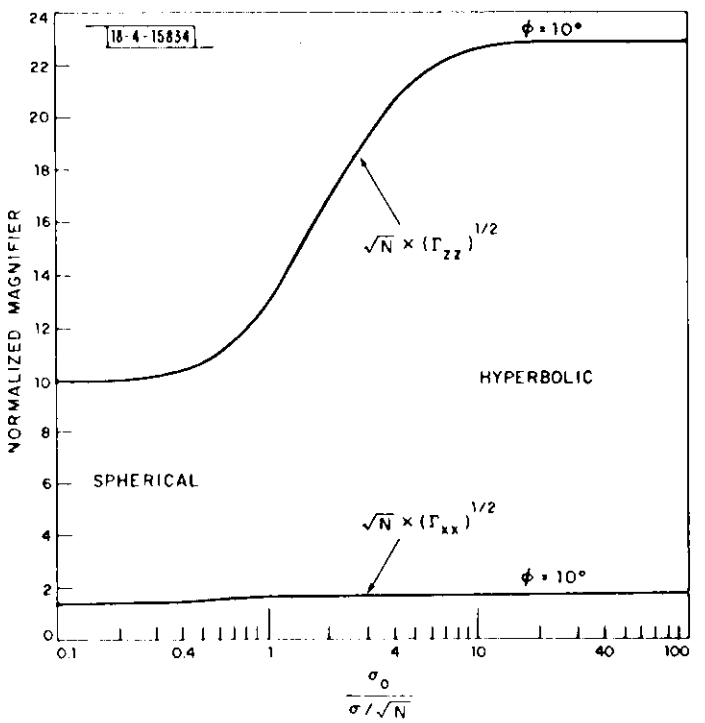

Figure 18.2

XIX. INDEPENDENT ALTITUDE MEASUREMENT

While spherical multilateration systems provide an altitude estimate, Sections XVI and XV show that the estimate normally is poor in the case of a ground based system, and can be poor in a satellite-based system for a sufficiently large clock error σ_0. Thus in some applications it may be desirable to use an independent altitude measurement (e.g., from a barometric altimeter) as an input to the position calculation algorithm so as to obtain an improved position estimate in all dimensions. The present section extends the analysis of Sections III - VIII to accommodate such a measurement.

Thus assume that measured altitude is to be used as an input to the calculation of subject position. Let (x',y',z') denote a Cartesian coordinate system centered at the subject, and oriented such that the z axis corresponds to altitude. In addition let

ζ = The altitude of the reference point (see Section VI) a above anaaltitude reference (e.g. sea level)

z^* = The measured altitude.

ε_z = The error in the measured altitude.

The quantities ζ, z^* and ε_z are related by the equation

$$z^* = \zeta + [0,0,-1]\,\underline{R} + \varepsilon_z \tag{19.1}$$

or equivalently

$$z^*/c = \frac{1}{c}\,\zeta + \frac{1}{c}\,[0,0,-1] \cdot \underline{R} + \varepsilon_z/c \tag{19.2}$$

The subject position now is to be estimated by "solving" (6.3) and (19.2) for $\underline{R}$ using the least squares procedure. The solution parallels that given in Section VI. The error in the resulting estimate is given by the expression

$$\hat{\underline{R}} - \underline{R} = c[\underline{F}_+' \underline{H}_+'(\underline{H}_+ \underline{P}_+ \underline{H}_+')^{-1} \underline{H}_+ \underline{F}_+]^{-1} \underline{F}_+ \underline{H}_+'(\underline{H}_+ \underline{P}_+\underline{H}_+')^{-1} \underline{H}_+ \underline{\varepsilon}_+ \quad (19.4)$$

where

$$\underline{\varepsilon}_+ = \begin{bmatrix} \underline{\varepsilon} \\ \varepsilon_z/c \end{bmatrix} \quad N+2 \qquad \underline{F}_+ = \begin{bmatrix} \underline{F} \\ 0,0,1 \end{bmatrix} \quad N+2 \quad (3)$$

$$\underline{H}_+ = \begin{bmatrix} \underline{H} & \begin{matrix} 0 \\ \vdots \\ 0 \end{matrix} \\ 0 \quad \cdots \quad 0 & 1 \end{bmatrix} \quad N+1 \quad (N+2) \qquad (19.5\text{-}7)$$

with $\underline{\varepsilon}$, $\underline{F}$ and $\underline{H}$ as in Section VI, and where $\underline{P}_+$ denotes the covariance matrix

$$\underline{P}_+ = E[\underline{\varepsilon}_+ \underline{\varepsilon}_+']$$

$$= \begin{bmatrix} \underline{P}_\varepsilon & \begin{matrix} 0 \\ \vdots \\ 0 \end{matrix} \\ 0 \quad \cdots \quad 0 & \sigma_z^2/c^2 \end{bmatrix} \qquad (19.8)$$

and $\underline{P}_{\varepsilon}$ denotes the covariance matrix of Section V.

The covariance matrix for the resulting positional errors is given by

$$\underline{P}_{\Delta R_+} = E[(\hat{\underline{R}} - \underline{R})(\hat{\underline{R}} - \underline{R})']$$

$$= c^2[\underline{F}_+' \underline{H}_+'(\underline{H}_+ \underline{P}_+ \underline{H}_+')^{-1} \underline{H} \underline{F}_+]^{-1} \tag{19.9}$$

The error magnification matrix defined by

$$\underline{\Gamma}_+ \stackrel{\Delta}{=} \frac{1}{(\sigma^* c)^2} \underline{P}_{\Delta R_+} \tag{19.10}$$

is as follows:

$$\underline{\Gamma}_+ = [\underline{F}_+' \underline{H}_+'(\underline{H}_+ \underline{P}_{N_+} \underline{H}_+')^{-1} \underline{H}_+ \underline{F}_+]^{-1} \tag{19.11}$$

where $\underline{P}_{N_+}$ denotes the normalized covariance matrix

$$\underline{P}_{N_+} = \begin{bmatrix} \underline{P}_N & 0 \\ 0 & \sigma_z^2/(\sigma^* c)^2 \end{bmatrix} \tag{19.12}$$

and $\underline{P}_N$ and $(\sigma^* c)^2$ are as in Section VII.

It is shown in Appendix III that the inverse of the covariance matrix (19.11) can be calculated as follows

$$\underline{\Gamma}_{+}^{-1} = \underline{L} + \begin{bmatrix} 0 & 0 & 0 \\ 0 & 0 & 0 \\ 0 & 0 & (\sigma^{*}c)^2/\sigma_z^2 \end{bmatrix} \tag{19.13}$$

where $\underline{L}$ is as in Section VIII.

Equation (19.13) shows that Γ_{+}^{-1} is computed exactly as in Section VIII except that the quantity $(\sigma^{*}c)^2/\sigma_z^2$ now must be added to the Z-Z element of $(\underline{\Gamma}_{+})^{-1}$. Thus the effect of the independent altitude measurement is to increase the Z-Z element of $\underline{\Gamma}^{-1}$ and correspondingly to reduce Γ_{zz}.

The effect of a highly accurate altitude measurement can be assessed by examining the limiting form of $\underline{\Gamma}_{+}$ as $\sigma_z \to 0$. It is clear from (19.13) that

$$\lim_{\sigma_z \to 0} \underline{\Gamma}_{+} = \begin{bmatrix} \begin{bmatrix} L_{xx} & L_{xy} \\ L_{xy} & L_{yy} \end{bmatrix}^{-1} & \begin{matrix} 0 \\ 0 \end{matrix} \\ \begin{matrix} 0 & 0 \end{matrix} & 0 \end{bmatrix} \tag{19.14}$$

Thus the error magnification factors $(\Gamma_{xx})_{+}$ and $(\Gamma_{yy})_{+}$ can be found from the expressions

$$(\Gamma_{xx})_{+} = \frac{L_{yy}}{L_{xx}L_{yy} - (L_{xy})^2} \tag{19.15}$$

$$(\Gamma_{yy})_{+} = \frac{L_{xx}}{L_{xx}L_{yy} - (L_{xy})^2} \tag{19.16}$$

where L_{xx}, L_{xy} and L_{yy} are calculated by the method of Section VIII. For small but non-vanishing σ_z it can be shown that the error magnification factor $(\Gamma_{zz})_+$ is given by

$$(\Gamma_{zz})_+ \approx \sigma_z^2/(\sigma^* c)^2 \qquad (19.17)$$

as expected.

XX. OPTIMUM BEACON CONSTELLATIONS

The following questions appear to be basic ones from the viewpoint of designing spherical multilateration systems.

1) What is the minimum total mean-squared positional error σ^2 that can be achieved from a given number N of beacons?

2) How should the beacons be deployed to achieve minimum error?

The present section answers these questions for beacon constellations satisfying the following restrictions.

Case I: The beacon locations are not restricted and $\sigma_0 > 0$.

Case II: The beacons are confined to a viewing cone having a half angle ϕ. Moreover, the system is ideal (i.e., $\sigma_0 = 0$).

The section also presents an example that illustrates the usefulness of the results.

Bounding arguments are used to identify the minimum errors and corresponding optimal constellations for Cases I and II. That is, a lower bound on σ^2 is established. Then it is shown that certain select constellations realize the bound.

The total mean-squared error σ^2 is given by the sum of the diagonal elements in the covariance matrix (7.2). That is,

$$\begin{aligned}\sigma^2 &= \sigma_x^2 + \sigma_y^2 + \sigma_z^2 \\ &= (\Gamma_{xx} + \Gamma_{yy} + \Gamma_{zz})\ (\sigma^*)^2 \end{aligned} \tag{20.1}$$

Thus the problem of minimizing σ^2 amounts to minimizing the error magnification factor

$$\frac{\sigma^2}{(\sigma^*)^2} = \Gamma_{xx} + \Gamma_{yy} + \Gamma_{zz} \tag{20.2}$$

The following bound[1] is used to deal with the quantity (20.2):

$$\Gamma_{xx} + \Gamma_{yy} + \Gamma_{zz} \geq \frac{1}{L_{xx}} + \frac{1}{L_{yy}} + \frac{1}{L_{zz}} \tag{20.3}$$

where the equal sign applies if and only if the $\underline{L}$ matrix is diagonal. The bound is useful in that it facilitates use of coordinate systems that do not necessarily diagonalize $\underline{L}$.

EXAMPLE 20.1 (Unrestricted Constellations)

Consider the problem of positioning N beacons in three dimensional space so as to minimize the total mean squared error σ^2 at the subject.

Let C denote any constellation of the N beacons. Let (x',y',z') denote an arbitrary Cartesian coordinate system located at the center of the unit sphere. Let (x,y,z) denote a Cartesian coordinate system located at the mass center of $m_0, m_1, \ldots m_N$, that differs from (x',y',z') only by a translation. Finally, let L_{xx}, L_{yy}, L_{zz} denote the diagonal elements of the $\underline{L}$ matrix for C, calculated in the coordinate system (x,y,z).

According to (20.2) and (20.3) the total mean-squared error σ^2 satisfies

$$\frac{\sigma^2}{(c\sigma^*)^2} \geq \frac{1}{L_{xx}} + \frac{1}{L_{yy}} + \frac{1}{L_{zz}} \tag{20.4}$$

[1] See Appendix I, Reference [1].

The parallel axis theorem of elementary mechanics asserts that

$$L_{xx} = \sum_{j=0}^{N} m_j (x_j)^2 = \sum_{j=0}^{N} m_j (x'_j)^2 - M(\overline{x'})^2$$

$$= M_H \overline{(x')^2} - M(\overline{x'})^2 \qquad (20.5)$$

where

$$M = \sum_{j=0}^{N} m_j \quad , \quad \overline{x'} = \frac{1}{M} \sum_{j=1}^{N} m_j \, x'_j \qquad (20.6\text{-}7)$$

$$M_H = \sum_{j=1}^{N} m_j \quad , \quad \overline{(x')^2} = \frac{1}{M_H} \sum_{j=1}^{N} m_j (x'_j)^2 \qquad (20.8\text{-}9)$$

Similarly

$$L_{yy} = M_H \overline{(y')^2} - M(\overline{y'})^2 \qquad (20.10)$$

$$L_{zz} = M_H \overline{(z')^2} - M(\overline{z'})^2 \qquad (20.11)$$

where

$$\overline{(y')^2} = \frac{1}{M_H} \sum_{j=1}^{N} m_j (y'_j)^2 \qquad (20.12)$$

$$\overline{(z')^2} = \frac{1}{M_H} \sum_{j=1}^{N} m_j (z'_j)^2 \qquad (20.13)$$

Use of (20.5), (20.10) and (20.11) in (20.4) yields

$$\frac{\sigma^2}{(c\sigma^*)^2} \geq \frac{1}{M_H\,\overline{(x')^2} - M(\overline{x^r})^2} + \frac{1}{M_H\overline{(y')^2} - M(\overline{y^r})^2}$$

$$+ \frac{1}{M_H\overline{(z')^2} - M(\overline{z^r})^2} \tag{20.14}$$

It follows from (20.14) that

$$\frac{\sigma^2}{(c\sigma^*)^2} \geq \frac{1}{M_H}\left[\frac{1}{\overline{(x')^2}} + \frac{1}{\overline{(y')^2}} + \frac{1}{\overline{(z')^2}}\right] \tag{20.15}$$

with equality possible only if $\overline{x^r} = \overline{y^r} = \overline{z^r} = 0$.

According to the Pythagorean Theorem, the coordinates (x_j', y_j', z_j') of each mass m_j on the unit sphere satisfy the relationship

$$(x_j')^2 + (y_j')^2 + (z_j')^2 = 1 \tag{20.16}$$

Summation of (20.16) gives

$$\sum_{j=1}^{N} m_j(x_j')^2 + \sum_{j=1}^{N} m_j(y_j')^2 + \sum_{j=1}^{N} m_j(z_j')^2 = \sum_{j=1}^{N} m_j \tag{20.17}$$

so that

$$\overline{(x')^2} + \overline{(y')^2} + \overline{(z')^2} = 1 \tag{20.18}$$

Use of (20.18) in (20.15) yields

$$\frac{\sigma^2}{(c\sigma^*)^2} \geq \frac{1}{M_H}\left[\frac{1}{\overline{(x')^2}} + \frac{1}{\overline{(y')^2}} + \frac{1}{1 - \overline{(x')^2} - \overline{(y')^2}}\right] \tag{20.19}$$

Straightforward minimization of the right hand-member of (20.19) over the domain defined by

$$\overline{(x')^2} + \overline{(y')^2} \leq 1 \tag{20.20}$$

$$0 \leq \overline{(x')^2} \quad , \quad 0 \leq \overline{(y')^2} \tag{20.21 a-b}$$

indicates that

$$\frac{\sigma^2}{(c\sigma^*)^2} \geq \frac{9}{M_H} \tag{20.22}$$

Moreover, the minimization procedure shows that equality in (20.22) holds only if $L_{xx} = L_{yy} = L_{zz} = M_H/3$.

A review of the development (20.1) - (20.22) shows that the lower bound (20.22) is achieved if and only if the following conditions are satisfied

1. The $\underline{L}$ matrix is diagonal.
2. $\overline{x'} = \overline{y'} = \overline{z'} = 0$.
3. $L_{xx} = L_{yy} = L_{zz} = M_H/3$.

For the case of equal ranging errors,

$$\sigma_1^2 = \sigma_2^2 = \ldots = \sigma_N^2 \tag{20.23}$$

The bound (20.22) reduces to

$$\frac{\sigma^2}{(c\sigma^*)^2} \geq 9/N \quad . \tag{20.24}$$

It is easy to identify beacon constellations that attain the bound (20.24). For example, for N = 4,6 the constellations shown in Figures 20.1 and 20.2 achieve the bound. Similarly, the N = 8, 12 and 20 constellations in which the beacon images are located at the vertices of the regular solids realize the bound (20.24). Also, any superposition of the "regular" constellations or their rotations achieve the bound (20.24). More generally, any constellation in which the beacon images are (approximately) uniformly distributed over the unit sphere satisfies conditions 1 - 3, and therefore (nearly) realizes the bound (20.24). Note that the bound (20.24) is equivalent to the relationship

$$\text{GDOP} \geq 3/\sqrt{N} \quad . \tag{20.25}$$

For the case of unequal ranging errors fewer constellations realize the lower bound (20.22) exactly. The bound can be realized approximately, however, by positioning the beacons so that m_1, m_2, ... m_N approximate a uniform distribution of mass over the unit sphere. For such constellations

$$\text{GDOP} \geq 3/\sqrt{M_H} \quad . \tag{20.26}$$

It is interesting to note that the bound (20.24) is identical to the corresponding bound for a hyperbolic system.[1] Thus an optimal spherical system is not more accurate than an optimal hyperbolic system having the same number of beacons. Rather the constellations have exactly the same accuracy.

END OF EXAMPLE

[1] See Example 11.2 of Reference [1].

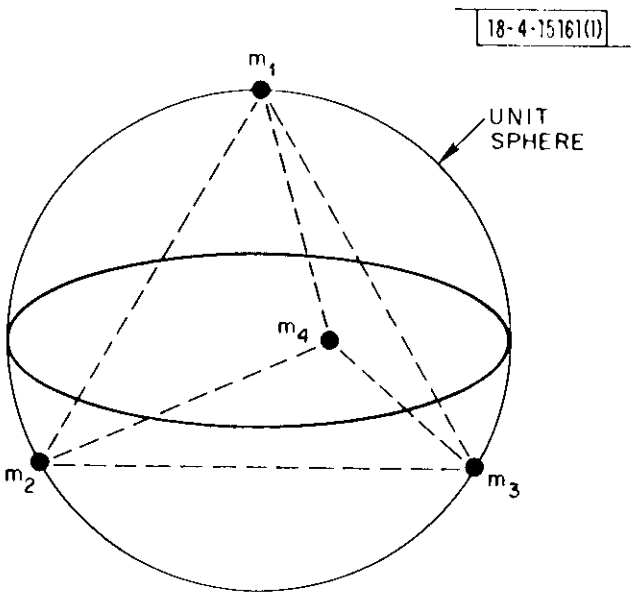

Figure 20.1

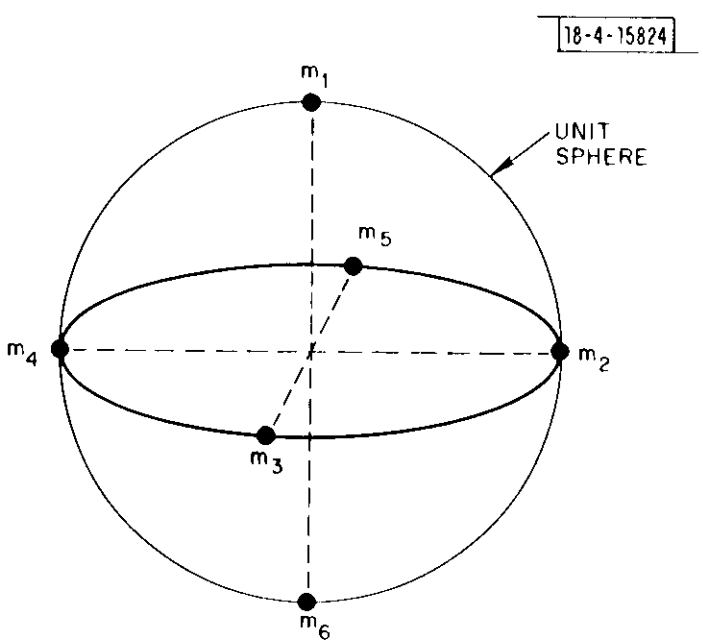

Figure 20.2

EXAMPLE 20.2 (Cone Restricted Constellation; $\sigma_0 = 0$)

Next consider the problem of placing N beacons within a cone of half angle ϕ so as to minimize the total mean-squared error σ^2 at the subject. Assume that the rms clock error σ_0 is zero.

Let (x, y, z) denote a Cartesian coordinate system at the center of the unit sphere and oriented such the z axis coincides with the cone axis as shown in Figure 20.3.

According to (20.2) and (20.3) σ^2 satisfies

$$\frac{\sigma^2}{(c\sigma^*)^2} \geq \frac{1}{L_{xx}} + \frac{1}{L_{yy}} + \frac{1}{L_{zz}} \tag{20.27}$$

On the basis of Figure 13.2 one expects that

$$L_{xx} << L_{zz} \qquad \text{and} \qquad L_{yy} << L_{zz} \tag{20.28-24}$$

so that the right hand-member of (20.27) is dominated by the $1/L_{xx}$ and $1/L_{yy}$ terms. This suggests that the proper strategy for minimizing $\sigma^2/(c\sigma^*)^2$ consists of placing the beacon images so as to maximize L_{xx} and L_{yy}. In the case of equal ranging errors

$$\sigma_1^2 = \sigma_2^2 = \ldots = \sigma_N^2 \tag{20.30}$$

or equivalently

$$m_1 = m_2 = \cdots = m_N = 1 \tag{20.31}$$

the quantities L_{xx} and L_{yy} evidently are maximized by placing the N beacon images uniformly around the ring R shown in Figure 20.4. A straightforward calculation shows that the associated $\underline{L}$ matrix is given by

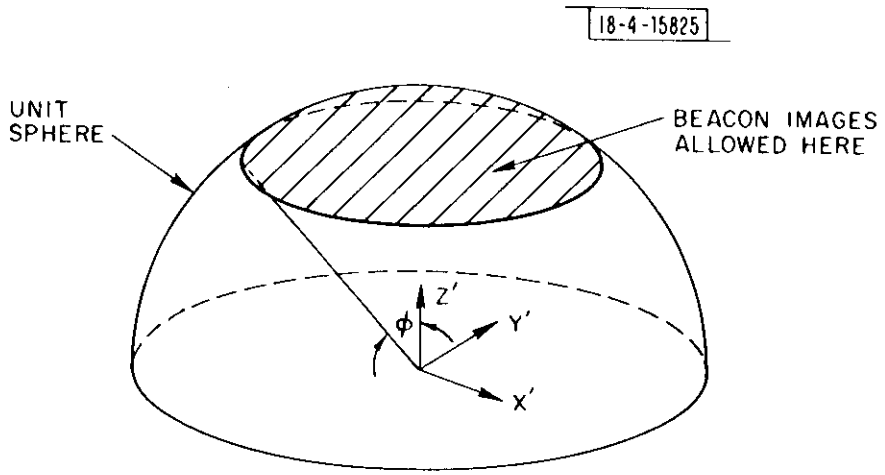

Figure 20.3

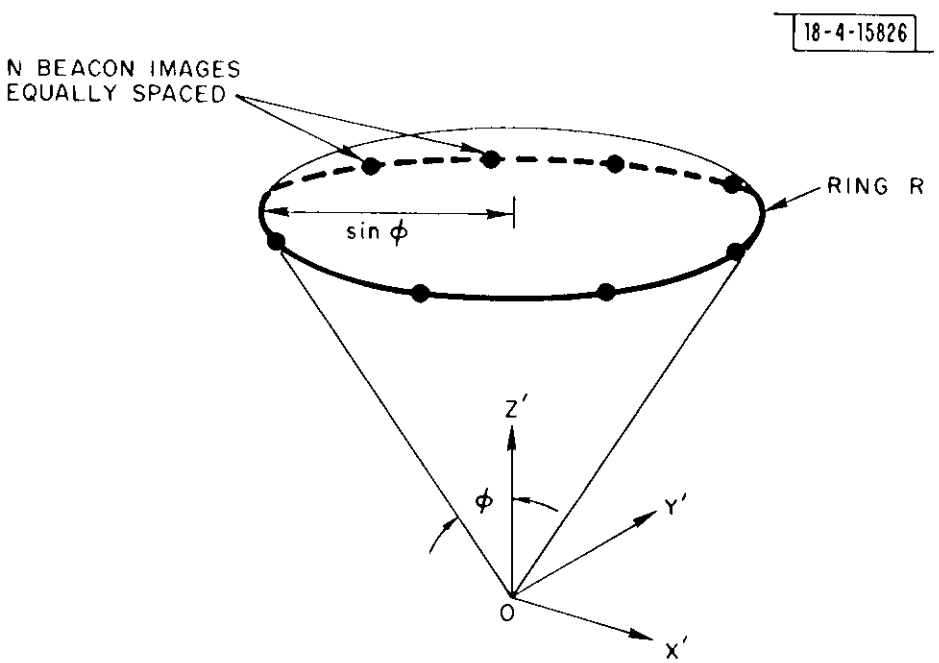

Figure 20.4

$$\underline{L} = N\begin{bmatrix} \frac{1}{2}\sin^2\phi & 0 & 0 \\ 0 & \frac{1}{2}\sin^2\phi & 0 \\ 0 & 0 & \cos^2\phi \end{bmatrix} \tag{20.32}$$

so that

$$\frac{\sigma^2}{(c\sigma^*)^2} = \frac{1}{N}\left[\frac{4}{\sin^2\phi} + \frac{1}{\cos^2\phi}\right] \tag{20.33}$$

and

$$GDOP = \frac{1}{\sqrt{N}}\left[\frac{4}{\sin^2\phi} + \frac{1}{\cos^2\phi}\right]^{1/2} \tag{20.34}$$

The conjecture that (20.33) actually is the minimum value of $\sigma^2/(c\sigma^*)^2$ can be explored as follows.

The quantities L_{xx}, L_{yy}, and L_{zz} are given by the expressions

$$L_{xx} = \sum_{j=0}^{N} m_j (x_j')^2 = M_H \overline{(x')^2} \tag{20.35}$$

$$L_{yy} = \sum_{j=0}^{N} m_j (y_j')^2 = M_H \overline{(y')^2} \tag{20.36}$$

$$L_{zz} = \sum_{j=0}^{N} m_j (z_j')^2 = M_H \overline{(z')^2} \tag{20.37}$$

where $\overline{(x')^2}$, $\overline{(y')^2}$ and $\overline{(z')^2}$ are as in (20.9), (20.12) and (20.13). Once again, the Pythagorean Theorem (20.18) applies. Use of (20.35), (20.36), and (20.37) in (20.27), followed by use of (20.18) to eliminate $(z')^2$ yields

$$\frac{\sigma^2}{(c\sigma^*)^2} \geq \frac{1}{M_H}\left[\frac{1}{\overline{(x')^2}} + \frac{1}{\overline{(y')^2}} + \frac{1}{1 - \overline{(x')^2} - \overline{(y')^2}}\right] \tag{20.38}$$

Now the coordinates x'_m, y'_j of any mass m_j within the cone satisfy

$$(x'_j)^2 + (y'_j)^2 = (r'_j)^2$$

$$\leq \sin^2 \phi \tag{20.39}$$

for $\phi \leq \pi/2$, with the equal sign possible only if m_j is on the ring R. Summation of (20.39) as in (20.17) shows that

$$\overline{(x'_j)^2} + \overline{(y'_j)^2} \leq \sin^2 \phi \tag{20.40}$$

for $\phi \leq \pi/2$, with the equal sign applying only if all of the masses $m_1, m_2, \ldots m_M$ are on R.

Minimization of the right-hand member of (20.38) over the domain D defined by (20.40) and the conditions

$$0 \leq \overline{(x'_j)^2} \quad , \quad 0 \leq \overline{(y'_j)^2} \tag{20.41-42}$$

produces a bound on $\sigma^2/(\sigma^* c)^2$ that depends only upon N and ϕ, and therefore one that can be compared with (20.33). The domain D consists of the shaded area in Figure 20.5. The minimization is performed most directly in terms of the variable

$$h = \overline{(x')^2} + \overline{(y')^2} \tag{20.43}$$

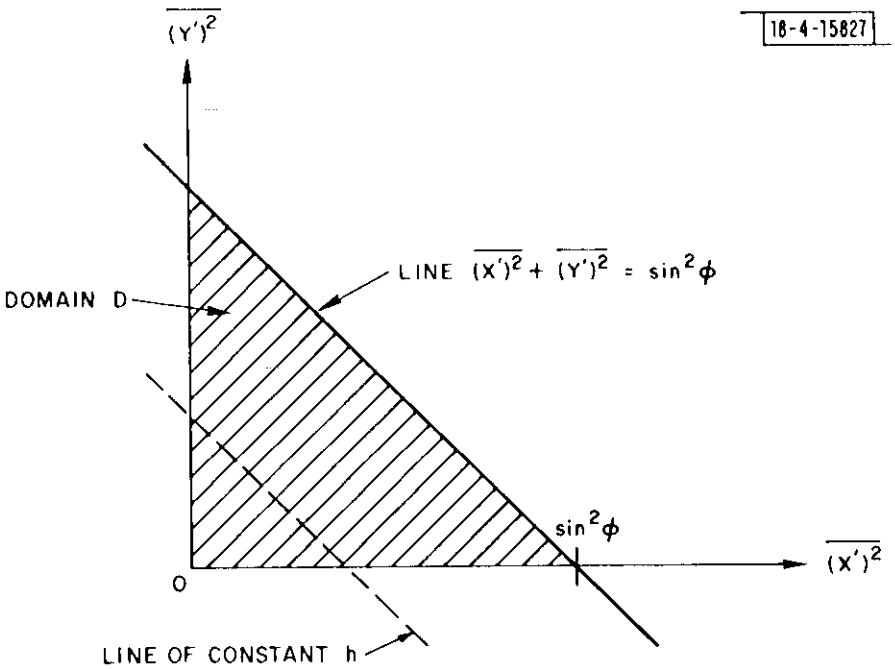
$\overline{(Y')^2}$
18-4-15827
LINE $\overline{(X')^2} + \overline{(Y')^2} = \sin^2\phi$
DOMAIN D
$\sin^2\phi$
$\overline{(X')^2}$
0
LINE OF CONSTANT h

Figure 20.5

Use of (20.43) in (20.38) gives

$$\frac{\sigma^2}{(\sigma^* c)^2} \geq \frac{1}{M_H}\left[\frac{1}{\overline{(x')^2}} + \frac{1}{h - \overline{(x')^2}} + \frac{1}{1-h}\right] \tag{20.44}$$

It follows successively from (20.44) that

$$\frac{\sigma^2}{(\sigma^* c)^2} \geq \frac{1}{M_H} \underset{0 \leq \overline{(x')^2} \leq h}{\text{Minimum}} \left[\frac{1}{\overline{(x')^2}} + \frac{1}{h - \overline{(x')^2}} + \frac{1}{1-h}\right]$$

$$= \frac{1}{M_H}\left[\frac{4}{h} + \frac{1}{1-h}\right]$$

$$\geq \frac{1}{M_H} \underset{0 \leq h \leq \sin^2\phi}{\text{Minimum}} \left[\frac{4}{h} + \frac{1}{1-h}\right]$$

$$= \begin{cases} \dfrac{1}{M_H}\left[\dfrac{4}{\sin^2\phi} + \dfrac{1}{\cos^2\phi}\right] & \text{for } \phi \leq \sin^{-1}\sqrt{2/3} \qquad (20.45) \\ \dfrac{9}{M_H} & \text{for } \phi > \sin^{-1}\sqrt{2/3} \qquad (20.46) \end{cases}$$

with equality in (20.45-46) possible only if

$$\overline{(x')^2} = \overline{(y')^2} = \frac{1}{2}\sin^2\phi \tag{20.47}$$

for $\phi \leq \sin^{-1}\sqrt{2/3}$, and only if

$$\overline{(x')^2} = \overline{(y')^2} = \overline{(z')^2} = \frac{1}{3} \tag{20.48}$$

for $\phi > \sin^{-1}\sqrt{2/3}$.

A review of the development (20.27) - (20.46) shows that the lower bound (20.45-46) is realized if, and only if, the following conditions are satisfied:

1. The $\underline{L}$ matrix is diagonal.
2. For $\phi \leq \sin^{-1}\sqrt{2/3}$ the masses m_j are located on the ring R in such a manner that (20.47) is satisfied.
3. For $\phi > \sin^{-1}\sqrt{2/3}$ the masses m_j are placed within the cone such that (20.48) is satisfied (but not necessarily on the ring R).

For the case (20.30), $M_H = N$. Thus Inequality (20.45) shows that for $\phi \leq \sin^{-1}\sqrt{2/3}$ the ratio $\sigma^2/(c\sigma^*)^2$ cannot be smaller than the value predicted by (20.33) and realized by the constellation of Figure 20.4. Inequality (20.46) indicates the limitations of (20.33). Specifically for $\phi > \sin^{-1}\sqrt{2/3}$, the ratio $\sigma^2/(c\sigma^*)^2$ <u>can</u> be smaller than that suggested by (20.33) but cannot be smaller than 9/N. Note that the constellation of Figure 20.4 with ϕ <u>equal to</u> $\sin^{-1}\sqrt{2/3}$, among others realizes the bound (20.46).

In the case of unequal ranging errors, the lower bound (20.45), (20.46) normally cannot be realized exactly. The bound (20.45) can be realized approximately for $\phi \leq \sin^{-1}\sqrt{2/3}$ by placing the beacon images $m_1, m_2, \ldots, m_N$ around the ring R so that conditions 1 and 2 are satisfied as nearly as possible. For $\phi > \sin^{-1}\sqrt{2/3}$, the bound (20.46) can be approximated by placing the beacon images $m_1, m_2, \ldots, m_N$ around a ring with $\phi = \sin^{-1}\sqrt{2/3}$ in such a manner that condition 1 and (20.48) are satisfied as nearly as possible.

For the case (20.30), Figure 20.6 depicts a normalized graph of the minimum value of GDOP versus ϕ, implied by (20.45-46). Note that GDOP achieves its absolute minimum at $\phi = \sin^{-1}\sqrt{2/3}$. Note also that the curve decreases more rapidly than the corresponding curve for a hyperbolic system,[1] but attains the same final value as predicted by Example 19.1.

---

[1] See Example 11.4 of Reference [9].

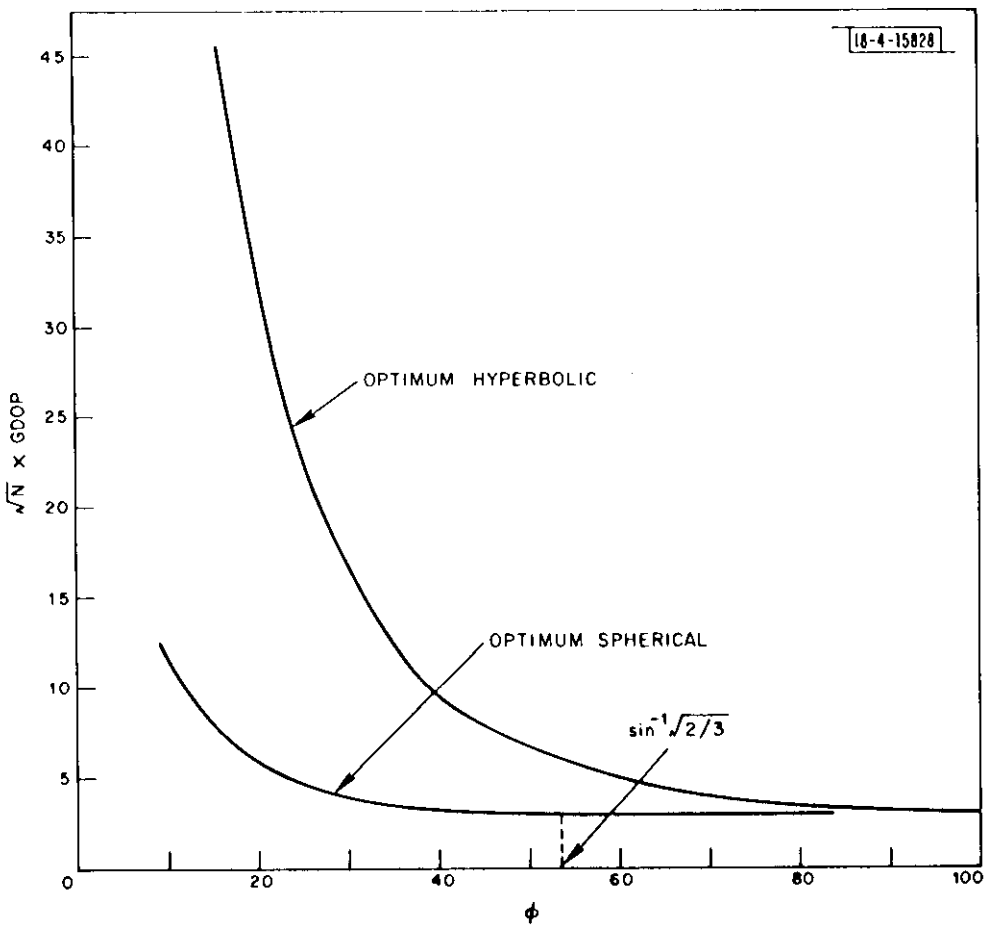
18-4-15828
45
40
35
30
25
20
15
10
5
0
20
40
60
80
100
$\sqrt{N} \times GDOP$
ϕ
OPTIMUM HYPERBOLIC
OPTIMUM SPHERICAL
$\sin^{-1}\sqrt{2/3}$

Figure 20.6

According to the discussion of Section X, the curves of optimum GDOP for non-ideal spherical systems lie between those shown in Figure 20.6.

END OF EXAMPLE

EXAMPLE 20.3 (Satellite Position Determination)

As an example of the application of the results of Example 20.2, consider the problem of determining the position of a satellite S in synchronous orbit about the earth. Assume that N ground stations simultaneously take range fixes to determine the position of S.

The earth subtends a half angle of 8.7° viewed from S. Thus the N ground stations are confined to a cone of half angle $\phi = 8.7°$.

If the "clock error" σ_0 is zero, then according to (20.45), the mean-squared positional error σ^2 is bounded below by

$$\sigma^2 \geq \frac{(\sigma^* c)^2}{M_H}\left[\frac{4}{\sin^2(8.7^o)} + \frac{1}{\cos^2(8.7^o)}\right]$$

$$= 229.7\ \frac{(\sigma^* c)^2}{M_H} \qquad (20.49)$$

If σ_0 is non-zero, then the mean-squared error σ^2 again satisfies (20.49) for the reasons given in Section X. Thus σ^2 satisfies (20.49) in any case.

For the parameter values

$$N = 3 \tag{20.50}$$

and

$$\sigma_1 = \sigma_2 = \sigma_3 = 30 \text{ nsec} \tag{20.51}$$

condition (20.49) shows that the rms positional error exceeds

$$\left[229.7 \frac{(30)^2}{3}\right]^{1/2} = 262 \text{ ft} \tag{20.52}$$

END OF EXAMPLE

REFERENCES

1. H.B. Lee, "Accuracy Limitations of Hyperbolic Multilateration Systems," Technical Note 1973-11, Lincoln Laboratory, M.I.T. (22 March 1973).

2. N. Marchand, "Error Distributions of Best Estimate of Position from Multiple Time Difference Hyperbolic Networks," IEEE Trans. Aerospace Navigational Electron. ANE-11, 96-900 (1964).

3. D. L. Snyder, "Navigation with High-Altitude Satellites: A Study of Errors in Position Determination," Technical Note 1967-11, Lincoln Laboratory, M.I.T. (6 February 1967), DDC AD-648828.

4. C.D. Sullivan, "Navigation with High-Altitude Satellites: A Study of the Effects of Satellite-User Geometry on Position Accuracy," Technical Note 1967-18, Lincoln Laboratory, M.I.T. (24 February 1967), DDC AD-651863.

5. T.J. Goblick and D.L. Snyder, "Analysis of Position Fix Accuracy Using High-Altitude Satellites," private communication.

6. G.W. Casserly and E.D. McConkey, "A Unified Approach to the Error Analysis of Position Finding Techniques," Univ. of Michigan; presented at the 14th Symposium on Advanced Navigational Techniques of the Avionics Panel of the Advisory Group for Aerospace Research and Development of NATO (AGARD), Milan, Italy (September 1967).

7. I.G. Stiglitz, et al., "Concept Formulation Studies of the Surveillance Aspects of the Fourth Generation Air Traffic Control System," Project Report ATC-7, Lincoln Laboratory, M.I.T. (21 September 1971).

8. D.C. Cooper, "Statistical Analysis of Position-Fixing; General Theory for Systems with Gaussian Errors," Proc. IEEE 119, 637-640 (1972).

9. E.J. Kelly, "The Use of Supplementary Receivers for Enhanced Positional Accuracy in the DAB System," Technical Note 1972-38, Lincoln Laboratory, M.I.T. (4 December 1972), DDC AD-756843.

10. F.N. David and J. Neyman, "Extension of the Markoff Theorem on Least Squares," Statistics Research Mem. 2, Dept. of Statistics, London (1938), 105-116.

APPENDIX I

PROOF OF IDENTITY (8.2)

Theorem:

If

$k > \ell$

$\underline{U}$ = any $k \times \ell$ matrix of rank ℓ

$\underline{H}$ = any $(k-\ell) \times k$ matrix of rank $(k-\ell)$ for which $\underline{H}\,\underline{U} = 0$

$\underline{P}$ = a $k \times k$ symmetric positive definite matrix

$\underline{M} = \underline{P}^{-1}$

Then

$$\underline{H}'\,(\underline{H}\,\underline{P}\,\underline{H}')^{-1}\,\underline{H} = [\underline{I} - \underline{M}\,\underline{U}(\underline{U}'\underline{M}\,\underline{U})^{-1}\underline{U}']\,\underline{M}[\underline{I} - \underline{U}(\underline{U}'\underline{M}\,\underline{U})^{-1}\underline{U}'\underline{M}] \qquad (A1.1)$$

Proof:

Let $\underline{H}_+$ denote the $k \times k$ matrix

$$\underline{H}_+ = \begin{bmatrix} \underline{H} \\ \underline{U}'\underline{M} \end{bmatrix} \begin{matrix} \updownarrow k-\ell \\ \updownarrow \ell \end{matrix} \qquad (A1.2)$$

Because of the way in which the final ℓ rows of $\underline{H}_+$ are constructed

$$(\underline{H}_+\,\underline{P}\,\underline{H}_+') = \left[\begin{array}{c|c} (\underline{H}\,\underline{P}\,\underline{H}') & 0 \\ \hline 0 & (\underline{U}'\,\underline{M}\,\underline{U}) \end{array}\right] \qquad (A1.3)$$

so that

$$(\underline{H}_+ \underline{P} \underline{H}_+')^{-1} = \left[\begin{array}{c|c} (\underline{H} \underline{P} \underline{H}')^{-1} & 0 \\ \hline 0 & (\underline{U}' \underline{M} \underline{U})^{-1} \end{array}\right] \tag{A1.4}$$

Thus

$$\underline{H}_+' (\underline{H}_+ \underline{P} \underline{H}_+')^{-1} \underline{H}_+ = [\underline{H}' \mid \underline{M} \underline{U}] \left[\begin{array}{c|c} (\underline{H} \underline{P} \underline{H}')^{-1} & 0 \\ \hline 0 & (\underline{U}' \underline{M} \underline{U})^{-1} \end{array}\right] \left[\begin{array}{c} \underline{H} \\ \hline \underline{U}' \underline{M} \end{array}\right]$$

$$= \underline{H}' (\underline{H} \underline{P} \underline{H}')^{-1} \underline{H} + \underline{M} \underline{U}(\underline{U}' \underline{M} \underline{U})^{-1} \underline{U}' \underline{M} \tag{A1.5}$$

Rearrangement of (A1.5) gives

$$\underline{H}' (\underline{H} \underline{P} \underline{H}')^{-1} \underline{H} = \underline{H}_+' (\underline{H}_+ \underline{P} \underline{H}_+')^{-1} \underline{H}_+ - \underline{M} \underline{U}(\underline{U}' \underline{M} \underline{U})^{-1} \underline{U}' \underline{M} \tag{A1.6}$$

But $\underline{H}_+' (\underline{H}_+ \underline{P} \underline{H}_+')^{-1} \underline{H}_+ = \underline{M}$. Consequently

$$\underline{H}' (\underline{H} \underline{P} \underline{H}')^{-1} \underline{H} = \underline{M} - \underline{M} \underline{U}(\underline{U}' \underline{M} \underline{U})^{-1} \underline{U}' \underline{M}$$

$$= [\underline{I} - \underline{M} \underline{U}(\underline{U}' \underline{M} \underline{U})^{-1} \underline{U}'] \underline{M} [\underline{I} - \underline{U}(\underline{U}' \underline{M} \underline{U})^{-1} \underline{U}' \underline{M}] \tag{A1.7}$$

Q.E.D.

APPENDIX II

DERIVATION OF EQUATION (12.3)

Outline of Derivation:

For any placement of the masses $(\sigma^*)^2/\sigma_1^2 \ldots (\sigma^*)^2/\sigma_N^2$ on the unit sphere, the matrix $\underline{L}$ of moments about the center of mass, the corresponding matrix $\underline{L}_0$ of moments about the origin, and the vector $\underline{\bar{r}}$ pointing from the origin to the center of mass satisfy the identity

$$\underline{L} = \underline{L}_0 - (m_0 + M_H)\, \underline{\bar{r}}\, \underline{\bar{r}}' \tag{A2.1}$$

where

$$M_H \triangleq \sum_{j=1}^{N} m_j \tag{A2.1a}$$

The identity is a form of the "parallel axis theorem" of elementary mechanics.

The relationship (12.3) is derived by averaging (A2.1) over all mass constellations that satisfy the following assumptions.

Assumptions

A1. The masses $(\sigma^*)^2/\sigma_1^2 \ldots (\sigma^*)^2/\sigma_N^2$ are confined to a region Ω on the surface of the unit sphere.

A2. The mass positions within Ω are uncorrelated and are described by identical probability density functions.

The derivation is broken into three steps. First the term $\underline{L}_0$ in (A2.1) is averaged over all mass constellations consistent with assumptions A1 and A2. Next the quantity $\underline{\bar{r}}\, \underline{\bar{r}}'$ is averaged over the same constellations. Finally the average of $\underline{L}$ is determined from the relationship

$$E[\underline{L}] = E[\underline{L}_0] - (m_0 + M_H)\, E[\underline{\bar{r}}\,\underline{\bar{r}}'] \qquad \text{(A2.2)}$$

where E denotes the expected value over the area Ω.

Step 1: Average of $\underline{L}_0$

Let (X', Y', Z') denote a Cartesian coordinate system centered at the origin. The expected value of $\underline{L}_0$ is as follows.

$$E[\underline{L}_0] = E\begin{bmatrix} \sum_{j=1}^{N} \left(\frac{\sigma^*}{\sigma_j}\right)^2 (X'_j)^2 & \sum_{j=1}^{N} \left(\frac{\sigma^*}{\sigma_j}\right)^2 X'_j Y'_j & \sum_{j=1}^{N} \left(\frac{\sigma^*}{\sigma_j}\right)^2 X'_j Z'_j \\ \sum_{j=1}^{N} \left(\frac{\sigma^*}{\sigma_j}\right)^2 X'_j Y'_j & \sum_{j=1}^{N} \left(\frac{\sigma^*}{\sigma_j}\right)^2 (Y'_j)^2 & \sum_{j=1}^{N} \left(\frac{\sigma^*}{\sigma_j}\right)^2 Y'_j Z'_j \\ \sum_{j=1}^{N} \left(\frac{\sigma^*}{\sigma_j}\right)^2 X'_j Z'_j & \sum_{j=1}^{N} \left(\frac{\sigma^*}{\sigma_j}\right)^2 Y'_j Z'_j & \sum_{j=1}^{N} \left(\frac{\sigma^*}{\sigma_j}\right)^2 (Z'_j)^2 \end{bmatrix}$$

$$= \sum_{j=1}^{N} \left(\frac{\sigma^*}{\sigma_j}\right)^2 E\left\{ \begin{bmatrix} X'_j \\ Y'_j \\ Z'_j \end{bmatrix} \begin{bmatrix} X'_j & Y'_j & Z'_j \end{bmatrix} \right\} \qquad \text{(A2.3)}$$

where X'_j, Y'_j, Z'_j denote coordinates of the mass $(\sigma^*/\sigma_j)^2$ measured from the origin. Since the probability density functions are identical for all masses, Eq. (A2.3) can be rewritten as follows

$$E[\underline{L}_0] = \left[\sum_{j=1}^{N} \left(\frac{\sigma^*}{\sigma_j}\right)^2\right] \times E\left\{\begin{bmatrix} X' \\ Y' \\ Z' \end{bmatrix} [X' \; Y' \; Z']\right\}$$

$$= M_H \times E\left\{\begin{bmatrix} X' \\ Y' \\ Z' \end{bmatrix} [X' \; Y' \; Z']\right\} \qquad \text{(A2.4)}$$

where X', Y', Z' denote the coordinates of a random point P within Ω having the same probability density function as the masses $(\sigma^*/\sigma_1)^2 \ldots (\sigma^*/\sigma_1)^2$.

Step 2: Average of $\underline{\bar{i}}\,\underline{\bar{i}}'$

The vector pointing from the origin to the center of mass is given by

$$\underline{\bar{i}} = \frac{1}{m_0 + M_H} \sum_{j=1}^{N} \left(\frac{\sigma^*}{\sigma_j}\right)^2 \begin{bmatrix} X'_j \\ Y'_j \\ Z'_j \end{bmatrix} \qquad \text{(A2.5)}$$

Thus the average value of the product $\underline{\bar{i}}\,\underline{\bar{i}}'$ can be expressed as follows.

$$E[\underline{\bar{i}}\,\underline{\bar{i}}'] = \frac{1}{(m_0 + M_H)^2} E\left\{\sum_{j=1}^{N}\sum_{k=1}^{N} \left(\frac{\sigma^*}{\sigma_j}\right)^2 \left(\frac{\sigma^*}{\sigma_k}\right)^2 \begin{bmatrix} X'_j \\ Y'_j \\ Z'_j \end{bmatrix} [X'_k \; Y'_k \; Z'_k]\right\} \qquad \text{(A2.6)}$$

It is convenient to break the right hand member of (A2.6) into two terms $\underline{I}_c$ and $\underline{I}_u$ as follows

$$E[\underline{\bar{i}}\ \underline{\bar{i}}'] = \underline{I}_c + \underline{I}_u \tag{A2.7}$$

where

$$\underline{I}_c = \frac{1}{(m_0 + M_H)^2} E\left\{ \sum_{j=1}^{N} \left(\frac{\sigma}{\sigma_j}\right)^{*4} \begin{bmatrix} X'_j \\ Y'_j \\ Z'_j \end{bmatrix} \begin{bmatrix} X'_j & Y'_j & Z'_j \end{bmatrix} \right\} \tag{A2.8}$$

$$\underline{I}_u = \frac{1}{(m_0 + M_H)^2} E\left\{ \sum_{j=1}^{N} \sum_{\substack{k=1 \\ j\neq k}}^{N} \left(\frac{\sigma}{\sigma_j}\right)^{*2} \left(\frac{\sigma}{\sigma_k}\right)^{*2} \begin{bmatrix} X'_j \\ Y'_j \\ Z'_j \end{bmatrix} \begin{bmatrix} X'_k & Y'_k & Z'_k \end{bmatrix} \right\} \tag{A2.9}$$

The term $\underline{I}_c$ contains all correlated products of mass coordinates.
The term $\underline{I}_u$ contains all uncorrelated products of mass coordinates.

The term $\underline{I}_c$ can be developed as follows

$$\underline{I}_c = \frac{1}{(m_0 + M_H)^2} \sum_{j=1}^{N} \left(\frac{\sigma}{\sigma_j}\right)^{*4} E\left\{ \begin{bmatrix} X'_j \\ Y'_j \\ Z'_j \end{bmatrix} \begin{bmatrix} X'_j & Y'_j & Z'_j \end{bmatrix} \right\}$$

$$= \frac{1}{(m_0 + M_H)^2} \left[\sum_{j=1}^{N} \left(\frac{\sigma}{\sigma_j}\right)^{*4} \right] xE\left\{ \begin{bmatrix} X' \\ Y' \\ Z' \end{bmatrix} \begin{bmatrix} X' & Y' & Z' \end{bmatrix} \right\} \tag{A2.10}$$

with the last line following from the hypothesis that the masses $(\sigma^*/\sigma_1)^2 \ldots (\sigma^*/\sigma_N)^2$ and the point P are described by identical probability density functions.

In a similar manner the term $\underline{T}_u$ can be developed as follows.

$$\underline{T}_u = \frac{1}{(m_0 + M_H)^2} \sum_{\substack{j=1 \\ j \neq k}}^{N} \sum_{k=1}^{N} \left(\frac{\sigma^*}{\sigma_j}\right)^2 \left(\frac{\sigma^*}{\sigma_k}\right)^2 E \left\{ \begin{bmatrix} X'_j \\ Y'_j \\ Z'_j \end{bmatrix} \begin{bmatrix} X'_k & Y'_k & Z'_k \end{bmatrix} \right\}$$

$$= \frac{1}{(m_0 + M_H)^2} \left[\sum_{\substack{j=1 \\ j \neq k}}^{N} \sum_{k=1}^{N} \left(\frac{\sigma^*}{\sigma_j}\right)^2 \left(\frac{\sigma^*}{\sigma_k}\right)^2 \right] \times \left\{ \begin{bmatrix} \overline{X}' \\ \overline{Y}' \\ \overline{Z}' \end{bmatrix} \begin{bmatrix} \overline{X}' & \overline{Y}' & \overline{Z}' \end{bmatrix} \right\}$$

$$= \frac{1}{(m_0 + M_H)^2} \left[M_H^2 - \sum_{j=1}^{N} \left(\frac{\sigma^*}{\sigma_j}\right)^4 \right] \times \left\{ \begin{bmatrix} \overline{X}' \\ \overline{Y}' \\ \overline{Z}' \end{bmatrix} \begin{bmatrix} \overline{X}' & \overline{Y}' & \overline{Z}' \end{bmatrix} \right\} \qquad \text{(A2.11)}$$

where the notation "————" denotes expected value.

Use of (A2.10) and (A2.11) in (A2.7) gives

$$E[\underline{\bar{i}}\ \underline{\bar{i}}'] = \frac{M_H^2}{(m_0 + M_H)^2} \begin{bmatrix} \bar{X}' \\ \bar{Y}' \\ \bar{Z}' \end{bmatrix} [\bar{X}'\ \bar{Y}'\ \bar{Z}']$$

$$+ \frac{\sum_{j=1}^{N} \left(\frac{\sigma^*}{\sigma_j}\right)^4}{(m_0 + M_H)^2} \times E \left\{ \begin{bmatrix} (X' - \bar{X}') \\ (Y' - \bar{Y}') \\ (Z' - \bar{Z}') \end{bmatrix} [(X' - \bar{X}')(Y' - \bar{Y}')(Z' - \bar{Z}')] \right\} \quad \text{(A2.12)}$$

Step 3: Average of $\underline{L}$

Substitution of (A2.4) and (A2.12) in (A2.2) gives

$$E[\underline{L}] = M_H \times E \left\{ \begin{bmatrix} X' \\ Y' \\ Z' \end{bmatrix} [X'\ Y'\ Z'] \right\}$$

$$- \frac{M_H^2}{(m_0 + M_H)} \begin{bmatrix} \bar{X}' \\ \bar{Y}' \\ \bar{Z}' \end{bmatrix} [\bar{X}'\ \bar{Y}'\ \bar{Z}']$$

$$- \frac{\sum_{j=1}^{N} \left(\frac{\sigma^*}{\sigma_j}\right)^4}{(m_0 + M_H)} \times E \left\{ \begin{bmatrix} (X' - \bar{X}') \\ (Y' - \bar{Y}') \\ (Z' - \bar{Z}') \end{bmatrix} [(X' - \bar{X}')(Y' - \bar{Y}')(Z' - \bar{Z}')] \right\} \quad \text{(A2.13)}$$

Equation (A2.13) can be rewritten as follows

$$E[\underline{L}] = \frac{m_0 M_H}{m_0 + M_H} \times E\left\{\begin{bmatrix} X' \\ Y' \\ Z' \end{bmatrix} [X' \; Y' \; Z']\right\}$$

$$+ \frac{1}{m_0 + M_H}\left[M_H^2 - \sum_{j=1}^{N} \left(\frac{\sigma^*}{\sigma_j}\right)^4\right] \times E\left\{\begin{bmatrix} (X' - \bar{X}') \\ (Y' - \bar{Y}') \\ (Z' - \bar{Z}') \end{bmatrix} [(X - \bar{X}')(Y - \bar{Y}')(Z - \bar{Z}')]\right\} \quad \text{(A2.14)}$$

Use of (A2.1a), (12.1) and (12.2) in (A2.14) leads directly to (12.3).

APPENDIX III

PROOF OF EQUATION (19.13)

The inverse of (19.11) is as follows

$$(\underline{\Gamma}_+)^{-1} = \underline{F}_+' \, \underline{H}_+' \, (\underline{H}_+ \, \underline{P}_{N_+} \, \underline{H}_+')^{-1} \, \underline{H}_+ \, \underline{F}_+ \tag{A3.1}$$

The matrix factor $\underline{H}_+' \, (\underline{H}_+ \, \underline{P}_{N_+} \, \underline{H}_+')^{-1} \, \underline{H}_+$ can be evaluated using the result of Appendix I as in Section VIII. Specifically, with the agreements

$$\underline{M}_+ = \underline{P}_{N_+}^{-1} \quad \text{and} \quad \underline{U}_+' = \underbrace{[-1,1,1\ldots1,0]}_{N+2} \tag{A3.2}$$

there follows

$$\underline{H}_+'(\underline{H}_+ \, \underline{P}_{N_+} \, \underline{H}_+')^{-1} \, \underline{H}_+ =$$

$$[\underline{I} - \underline{M}_+ \, \underline{U}_+(\underline{U}_+' \, \underline{M}_+ \, \underline{U}_+)^{-1} \, \underline{U}_+'] \, \underline{M}_+[\underline{I} - \underline{U}_+(\underline{U}_+' \, \underline{M}_+ \, \underline{U}_+)^{-1} \, \underline{U}_+' \, \underline{M}_+] \tag{A3.3}$$

Use of (A3.3) in (A3.1) shows that

$$(\underline{\Gamma}_+)^{-1} = \underline{K}_+' \, \underline{M}_+ \, \underline{K}_+ \tag{A3.4}$$

where

$$\underline{K}_+ = [\underline{I} - \underline{U}_+(\underline{U}_+' \, \underline{M}_+ \, \underline{U}_+)^{-1} \, \underline{U}_+' \, \underline{M}_+] \, \underline{F}_+ \tag{A3.5}$$

Evaluation of $\underline{K}_+$ shows that

$$\underline{K}_+ = \begin{bmatrix} \underline{K} \\ 0\ 0\ 1 \end{bmatrix} \tag{A3.6}$$

where $\underline{K}$ is as in Section VIII. Consequently, the matrix $(\underline{\Gamma}_+)^{-1}$ is given by

$$(\underline{\Gamma}_+)^{-1} = \begin{bmatrix} \underline{K}' \\ 0\ 0\ 1 \end{bmatrix} \begin{bmatrix} \underline{M} & 0 \\ 0 & (\sigma^*c)^2/\sigma_z^2 \end{bmatrix} \begin{bmatrix} \underline{K} \\ 0\ 0\ 1 \end{bmatrix}$$

$$= \underline{K}'\ \underline{M}\ \underline{K} + \begin{bmatrix} 0 & 0 & 0 \\ 0 & 0 & 0 \\ 0 & 0 & (\sigma^*c)^2/\sigma_z^2 \end{bmatrix}$$

$$= \underline{L} + \begin{bmatrix} 0 & 0 & 0 \\ 0 & 0 & 0 \\ 0 & 0 & (\sigma^*c)^2/\sigma_z^2 \end{bmatrix} \tag{A3.7}$$

where $\underline{L}$ is as in Section VIII.

Q.E.D.